Preprint No. xxxx, Department of Mathematics, University of Utrecht, April 2007.

# FINITE ELEMENT WAVELETS WITH IMPROVED QUANTITATIVE PROPERTIES

HOANG NGUYEN AND ROB STEVENSON

Abstract. In [DS99c], finite element wavelets were constructed on polygonal domains or Lipschitz manifolds that are piecewise parametrized by mappings with constant Jacobian determinants. The wavelets could be arranged to have any desired order of cancellation properties, and they generated stable bases for the Sobolev spaces $H^s$ for $|s| < \frac{3}{2}$ (or $|s| \leq 1$ on manifolds). Unfortunately, it appears that the quantitative properties of these wavelets are rather disappointing. In this paper, we modify the construction from [DS99c] to obtain finite element wavelets which are much better conditioned.

## 1. Introduction

The use of wavelets bases for solving operator equations, as partial differential equations and (boundary) integral equations, has a number of advantages. Firstly, when applying suitable wavelets, stiffness matrices resulting from Galerkin discretizations are well-conditioned uniformly in their sizes, allowing for efficient iterative solutions. Secondly, when the wavelets have cancellation properties of sufficiently high order, stiffness matrices of integral operators can be compressed to truly sparse matrices without reducing the convergence rate, resulting in a method of optimal computational complexity (cf. [Sch98]). Thirdly, adaptive wavelet methods can be applied that convergence with the rate of best $N$-term approximations from the wavelet basis for the underlying Sobolev space, in linear complexity ([CDD01, CDD02]) For an overview of wavelets and their applications in numerical analysis, see [Dah97, Coh03].

A bottleneck for the applications of wavelets to solving operator equations is their construction on general domains or manifolds on which these equations are formulated. Traditionally, wavelets are constructed in a shift- and scale invariant setting using Fourier techniques, yielding wavelet bases on $\mathbb{R}^n$ or on tori, cf. [Dau92, CDF92].

The construction of biorthogonal wavelets on the interval in [DKU99] (see also [CQ92, CDV93]), as well as the Fourier-free theoretical framework in [Dah96, CDP96], opened a way to construct wavelets on general domains or manifolds using domain decomposition techniques. The domain or manifold under consideration is thought as a disjoint union of patches, each of them being some parametric image of the $n$-cube. On the $n$-cube, wavelets are easily constructed from the wavelets on the interval by tensor products. Roughly

*Date*: April 16, 2007.

2000 *Mathematics Subject Classification.* 65T60, 65N30, 65F35, 65R20.

*Key words and phrases.* finite elements, wavelets, Riesz bases, cancellation properties, partial differential equations, boundary integral equations.

speaking, the technique now consists of lifting the wavelets on the $n$-cube to the patches, after which they are 'glued' over the interfaces, see e.g. [DS99a]. For related approaches, see [DS99b, CTU99, CTU00, CM00, KS06, HS06]. A common property of these approaches is that they all yield tensor product-based wavelets.

An alternative construction of wavelets on polygonal domains was proposed in [Ste98, DS99c]. Here, the idea is to construct wavelet bases for standard Lagrange finite element spaces. A price to be paid for the flexibility of this approach is that the dual wavelets are globally supported. However, this is not a drawback for solving operator equations, since the dual wavelets do not enter the algorithms. A modified construction was proposed in [Ste03] yielding locally supported dual wavelets, and so allowing finite element wavelets to be used also in other applications. Unfortunately, it appears that the quantitative properties of the wavelets constructed in [DS99c] are rather disappointing. In this paper, we modify the construction from [DS99c] to obtain finite element wavelets which are much better conditioned. Although we restrict ourselves to the construction of wavelets on polygonal domains, the same technique applies to the construction of wavelets on Lipschitz manifolds that are piecewise parametrized by mappings having constant Jacobian determinants. Adaptations of the construction required for handling more general domains or manifolds are discussed in [Ste07]. Other finite element wavelets on domains have been presented in, e.g., [KO95, FQ00, CES00].

The outline of this paper is as follows: In the rest of this section, we specify our notations. In Section 2, we develop a theoretical framework which identifies in which way the available freedom in the construction can be used to optimize the condition numbers of the wavelet bases. In Section 3, we apply this framework to obtain concrete realizations of finite element wavelets. The resulting wavelet bases turn out to be very well conditioned, and in comparison to the original construction, their condition numbers are up to a factor thousand smaller as confirmed by numerical results in Section 4. Coefficients of wavelets obtained with our construction are collected in the appendix.

We begin with some basic notations and definitions which will be used throughout this paper. First of all, to make the notations not unnecessarily complicated, we will drop references to the underlying domain or index sets whenever there is no risk of confusion, i.e., we will write $L^2$ for $L^2(\Omega)$ etc. In order to avoid repeated use of generic but unspecified constants, by $C \lesssim D$ we mean that $C$ can be bounded by a multiple of $D$, independently of parameters on which $C$ and $D$ may depend. Obviously, $C \gtrsim D$ means $D \lesssim C$, and $C \eqsim D$ means $C \lesssim D$ and $C \gtrsim D$.

For $s \geq 0$, $H^s$ will denote a Sobolev space on $\Omega$, possibly incorporating (essential) boundary conditions, where $\Omega$ is an $n$-dimensional domain. For $s < 0$, $H^s$ will be the dual of $H^{-s}$, i.e., $H^s = (H^{-s})'$, and $(H^0)' = H^0 = L^2$, i.e., $L^2$ is chosen to be the pivot space. This choice allows us to use the notation $\langle f, x\rangle_{L^2}$ both for $f, x \in L^2$ as well as for $f \in H^{-s}$, $x \in H^s$, meaning either $f(x)$ if $s \geq 0$ or $x(f)$ if $s < 0$. Further, $\langle\cdot,\cdot\rangle_{H^s}$ and $\|\cdot\|_{H^s}$ will denote the inner product and the (induced) norm on $H^s$, respectively, whereas $\|\cdot\|_{H^s\to H^t}$ will denote the (induced) operator norm on the space of bounded linear operators from $H^s$ to $H^t$. Unless stated otherwise, $\langle\cdot,\cdot\rangle$ and $\|\cdot\|$ will denote some canonical inner product and norm, e.g., the Euclidean inner product, the spectral norm, the $L^2$-norm, etc..

We will adopt the following compact notations from the literature (cf. [Dah97]). For $\Sigma$ being a countable collection of functions in some separable Hilbert space $H$, equipped with some inner product $\langle\cdot,\cdot\rangle_H$ and norm $\|\cdot\|_H$, we will formally identify $\Sigma$ with a column vector (of functions in $H$). For $\mathbf{c} = (c_\sigma)_{\sigma\in\Sigma}$ being a column vector of scalars, $\mathbf{c}^T\Sigma$ will denote the formal series $\sum_{\sigma\in\Sigma} c_\sigma\sigma$; and likewise for $\mathbf{C} = (c_{\tau,\sigma})_{\tau,\sigma\in\Sigma}$ being a matrix, $\mathbf{C}\Sigma$ will denote the collection $(\sum_{\sigma\in\Sigma} c_{\tau,\sigma}\sigma)_{\tau\in\Sigma}$, again viewed as a column vector.

A collection $\Sigma$ is called a *Riesz system* (in $H$) if

$$\|\mathbf{c}^T\Sigma\|_H \eqsim \|\mathbf{c}\| \qquad (\mathbf{c}\in l_2(\Sigma)),$$

where $l_2(\Sigma) := \big\{\mathbf{c} = (c_\sigma)_{\sigma\in\Sigma} : \|\mathbf{c}\| = \|\mathbf{c}\|_{l_2(\Sigma)} := \big(\sum_{\sigma\in\Sigma} c_\sigma^2\big)^{\frac{1}{2}} < \infty\big\}$. For such a system, we let

$$\Lambda_\Sigma = \Lambda_{\|\cdot\|_H,\Sigma} := \sup_{\mathbf{c}\in l_2(\Sigma)} \frac{\|\mathbf{c}^T\Sigma\|_H^2}{\|\mathbf{c}\|^2} \quad\text{and}\quad \lambda_\Sigma = \lambda_{\|\cdot\|_H,\Sigma} := \inf_{\mathbf{c}\in l_2(\Sigma)} \frac{\|\mathbf{c}^T\Sigma\|_H^2}{\|\mathbf{c}\|^2},$$

and we define its *condition number* $\kappa_\Sigma$ by

$$\kappa_\Sigma = \kappa_{\|\cdot\|_H,\Sigma} = \frac{\Lambda_\Sigma}{\lambda_\Sigma}.$$

In addition, if such a system is a basis for $H$ then it is called a *Riesz basis*. Given a sequence of Riesz systems $(\Sigma_l)_l$, $\Sigma_l$ are said to be *uniform Riesz systems* if $\sup_l \Lambda_{\Sigma_l} < \infty$ and $\inf_l \lambda_{\Sigma_l} > 0$.

As a generalization, let $(\mathcal{W}_l)_l$ be a sequence of subspaces of $H$, now generally more than one dimensional, such that

$$\|\sum_l w_l\|_H^2 \eqsim \sum_l \|w_l\|_H^2 \qquad (w_l\in\mathcal{W}_l).$$

The *condition number* $\kappa_{(\mathcal{W}_l)_l}$ of $(\mathcal{W}_l)_l$, sometimes called the *condition number of the decomposition* of the sum $\sum_l \mathcal{W}_l$ into its components, denoted as $\kappa_{(\mathcal{W}_l)_l}$ or as $\kappa_{\|\cdot\|_H,(\mathcal{W}_l)_l}$ in case confusion is possible, is defined by

$$\kappa_{(\mathcal{W}_l)_l} = \kappa_{\|\cdot\|_H,(\mathcal{W}_l)_l} = \frac{\displaystyle\sup_{\{(w_l)_l : w_l\in\mathcal{W}_l\}} \frac{\|\sum_l w_l\|_H^2}{\sum_l \|w_l\|_H^2}}{\displaystyle\inf_{\{(w_l)_l : w_l\in\mathcal{W}_l\}} \frac{\|\sum_l w_l\|_H^2}{\sum_l \|w_l\|_H^2}}.$$

With $\Psi_l$ being some uniform Riesz bases for $\mathcal{W}_l$, from above definitions one may verify that

$$\frac{\inf_l \lambda_{\Psi_l}}{\sup_l \Lambda_{\Psi_l}}\, \kappa_{(\mathcal{W}_l)_l} \le \kappa_{\cup_l \Psi_l} \le \frac{\sup_l \Lambda_{\Psi_l}}{\inf_l \lambda_{\Psi_l}}\, \kappa_{(\mathcal{W}_l)_l} \tag{1.1}$$

(cf. [Ngu05, §2.1]).

For $\Sigma$ and $\tilde{\Sigma}$ being two countable collections of functions in $H^{-s}$ and $H^s$, respectively, $\langle\Sigma,\tilde{\Sigma}\rangle_{L^2}$ will denote the matrix $(\langle\sigma,\tilde{\sigma}\rangle_{L^2})_{\sigma\in\Sigma,\tilde{\sigma}\in\tilde{\Sigma}}$, and so, for $\mathbf{A}$ and $\tilde{\mathbf{A}}$ being two matrices of appropriate dimensions, $\langle\mathbf{A}\Sigma,\tilde{\mathbf{A}}\tilde{\Sigma}\rangle_{L^2} = \mathbf{A}\langle\Sigma,\tilde{\Sigma}\rangle_{L^2}\tilde{\mathbf{A}}^T$.

## 2. General construction principles

Based on the theory in [DS99c], in this section we develop a theoretical framework which identifies in which way the available freedom in the wavelet construction can be used to optimize the condition numbers of the wavelet bases.

### 2.1. Biorthogonal space decompositions and wavelets.

We begin with recalling a general principle for the construction of biorthogonal wavelets, that, properly scaled, generate Riesz bases for a range of Sobolev spaces, which starts with the construction of biorthogonal space decompositions.

**Theorem 2.1** (biorthogonal space decompositions, [DS99c]). *Consider the following two multiresolution analyses*

$$V_0 \subset V_1 \subset \cdots \subset L^2, \text{ with } \operatorname{clos}_{L^2}(\cup_{j\geq 0} V_j) = L^2$$
$$\tilde{V}_0 \subset \tilde{V}_1 \subset \cdots \subset L^2, \text{ with } \operatorname{clos}_{L^2}(\cup_{j\geq 0} \tilde{V}_j) = L^2.$$

*Suppose that*

($\mathcal{Q}$) $\exists$ *uniformly bounded projectors, called* biorthogonal projectors, $Q_j : L^2 \to L^2$ *such that*
$$\operatorname{Im} Q_j = V_j,\ \operatorname{Im}(I - Q_j) = \tilde{V}_j^{\perp_{L^2}},$$
*or equivalently for their $L^2$-adjoints*
$$\operatorname{Im} Q_j^* = \tilde{V}_j,\ \operatorname{Im}(I - Q_j^*) = V_j^{\perp_{L^2}}.$$

($\mathcal{J}$) *both sequences satisfy* Jackson estimates *with parameters $d > 0$, $\tilde{d} > 0$ uniformly in $j$, i.e.,*
$$\inf_{v_j \in V_j} \|v - v_j\|_{L^2} \lesssim 2^{-jd}\|v\|_{H^d} \qquad (v \in H^d),$$
$$\inf_{\tilde{v}_j \in \tilde{V}_j} \|v - \tilde{v}_j\|_{L^2} \lesssim 2^{-j\tilde{d}}\|v\|_{H^{\tilde{d}}} \qquad (v \in H^{\tilde{d}}).$$

($\mathcal{B}$) *both sequences satisfy* Bernstein estimates *with parameters $0 < \gamma < d$, $0 < \tilde{\gamma} < \tilde{d}$ uniformly in $j$, i.e., for every $s \in [0, \gamma)$ and $\tilde{s} \in [0, \tilde{\gamma})$, it holds that*
$$\|v_j\|_{H^s} \lesssim 2^{js}\|v_j\|_{L^2} \qquad (v_j \in V_j),$$
$$\|\tilde{v}_j\|_{H^{\tilde{s}}} \lesssim 2^{j\tilde{s}}\|\tilde{v}_j\|_{L^2} \qquad (\tilde{v}_j \in \tilde{V}_j).$$

*Then, for every $s \in (-\tilde{d}, \gamma)$ and $t \in (-\tilde{\gamma}, d)$, with $Q_{-1} := 0$,*

$$(\mathcal{R}1) \quad \left\{ \begin{array}{lll} \|\sum_{j=-1}^{\infty} w_j\|_{H^s}^2 & \lesssim \sum_{j=-1}^{\infty} 4^{js}\|w_j\|_{L^2}^2 & (w_j \in \operatorname{Im}(Q_{j+1} - Q_j)) \\ \sum_{j=-1}^{\infty} 4^{jt}\|(Q_{j+1} - Q_j)u\|_{L^2}^2 & \lesssim \|u\|_{H^t}^2 & (u \in H^t). \end{array} \right.$$

*For every $s \in (-\tilde{\gamma}, \gamma)$, the mappings $(w_j)_j \mapsto \sum_{j=-1}^{\infty} w_j$ and $u \mapsto ((Q_{j+1} - Q_j)u)_j$, which are bounded in the sense of ($\Re 1$), are each others inverse. Thus, for every $s \in (-\tilde{\gamma}, \gamma)$,*

$$(\Re 2) \qquad \|u\|_{H^s}^2 \eqsim \sum_{j=-1}^{\infty} 4^{js} \|(Q_{j+1} - Q_j)u\|_{L^2}^2 \qquad (u \in H^s).$$

*Analogous results ($\Re 1^*$) and ($\Re 2^*$) are valid at the dual side, i.e., with interchanged roles of $(Q_j, d, \gamma)$ and $(Q_j^*, \tilde{d}, \tilde{\gamma})$. The decompositions $L^2 = \oplus_{j \geq -1} \mathrm{Im}(Q_{j+1} - Q_j)$ and $L^2 = \oplus_{j \geq -1} \mathrm{Im}(Q_{j+1}^* - Q_j^*)$ are called* biorthogonal space decompositions*.*

As a direct consequence of Theorem 2.1, we obtain:

**Corollary 2.2.** *For $j \geq -1$ and $J_j$ being some index set, let*

$$\Psi_j = \{\psi_{j,x} : x \in J_j\},$$

*whose elements are called* wavelets, *be uniform $L^2$-Riesz bases for the* detail spaces

$$V_{j+1} \cap \tilde{V}_j^{\perp_{L^2}} = \mathrm{Im}(Q_{j+1} - Q_j),$$

*where $Q_{-1} = 0$ as before and $\tilde{V}_{-1} := \{0\}$. Then, for $s \in (-\tilde{\gamma}, \gamma)$, the collection*

$$\bigcup_{j=-1}^{\infty} 2^{-js} \Psi_j$$

*is a Riesz basis for $H^s$.*

In the following, we will construct a pair of multiresolution analyses $(V_j)_j$ and $(\tilde{V}_j)_j$ satisfying all assumptions mentioned above as well as uniformly local bases $\Psi_j$ for the detail spaces $V_{j+1} \cap \tilde{V}_j^{\perp_{L^2}}$. The verification of Jackson and Bernstein estimates can follow standard lines, and it is usually not a problem to equip $V_0$ with an $L^2$-Riesz basis. Therefore, we will focus on the *existence of the biorthogonal projectors $Q_j$ and on the construction of the $\Psi_j$ for $j \geq 0$.*

## 2.2. **Projectors and angles between spaces.**

In this subsection, we derive an upper bound for the $L^2$-condition number of a wavelet basis $\Psi_j$ for $V_{j+1} \cap \tilde{V}_j^{\perp_{L^2}}$ in terms of angles between several spaces and the $L^2$-condition number of some auxiliary Riesz system in $V_{j+1}$. We start with a lemma (for its proof, see [Ste03]):

**Lemma 2.3** (Lemma 2.1, [Ste03])**.** *For some $\Omega \subset \mathbb{R}^n$, let $\breve{V}$ and $\tilde{V}$ be closed subspaces of $L^2 = L^2(\Omega)$ equipped with inner product $\langle \cdot, \cdot \rangle = \langle \cdot, \cdot \rangle_{L^2}$ and norm $\| \cdot \| = \| \cdot \|_{L^2}$.*

(a) *The following statements are equivalent:*
   (i) *There exist Riesz bases $\breve{\Sigma}$ and $\tilde{\Sigma}$ for $\breve{V}$ and $\tilde{V}$ such that $\mathbf{M} := \langle \breve{\Sigma}, \tilde{\Sigma} \rangle$ is boundedly invertible. A sufficient condition is that $\Re \mathbf{M} := \frac{1}{2}(\mathbf{M} + \mathbf{M}^*) > 0$.*

(ii)

$$\inf_{0\neq\tilde v\in\tilde V}\sup_{0\neq\breve v\in\breve V}\frac{|\langle\tilde v,\breve v\rangle|}{\|\tilde v\|\|\breve v\|}>0$$

*and*

$$\inf_{0\neq\breve v\in\breve V}\sup_{0\neq\tilde v\in\tilde V}\frac{|\langle\tilde v,\breve v\rangle|}{\|\tilde v\|\|\breve v\|}>0.$$

(iii) *There exists a (unique) bounded projector $P: L^2\to L^2$ with $\operatorname{Im}P=\breve V$ and $\operatorname{Im}(I-P)=\tilde V^\perp$, i.e., a biorthogonal projector. Moreover, $P_{|_{\tilde V}}$ is invertible.*

(iv) *To any Riesz basis for $\tilde V$ there corresponds a unique dual collection in $\breve V$. Moreover, this collection is a Riesz basis for $\breve V$.*

*If any of (i)–(iv) is valid, then*

$$Px=\langle x,\tilde\Sigma\rangle\langle\breve\Sigma,\tilde\Sigma\rangle^{-1}\breve\Sigma\qquad(x\in L^2).$$

(b) *Let any of the equivalent conditions (i)-(iv) from (a) be satisfied. Let $X$, $\breve W$ be subspaces of $L^2$ such that $X=\breve W+\breve V$ and*

$$\cos\angle(\breve W,\breve V):=\sup_{0\neq\xi\in\breve W,0\neq\breve v\in\breve V}\frac{|\langle\xi,\breve v\rangle|}{\|\xi\|\|\breve v\|}<1.$$

*Then $(I-P)_{|_{\breve W}}:\breve W\to X\cap\tilde V^\perp$ is boundedly invertible, see Figure 1.*

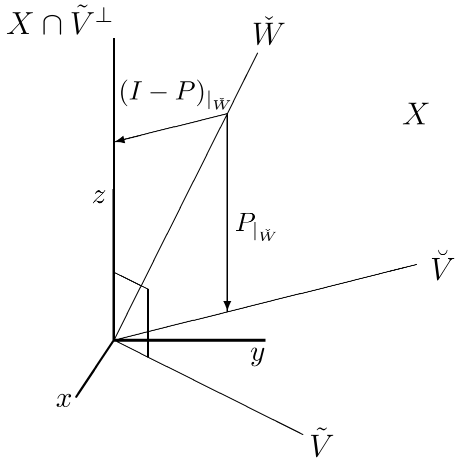


FIGURE 1. Illustration for Lemma 2.3(b). $L^2$ and $X$ are represented by $\mathbb{R}^3$ and the plane $x=0$, respectively. $\tilde V$ is contained in the plane $z=0$.

**Remark 2.4.** *If, in Lemma 2.3,*

- *the pair $(\breve V,\tilde V)$ and the two spaces $X$ and $\breve W$ are replaced by a sequence of pairs of closed subspaces $(\breve V_j,\tilde V_j)_j$ and two sequences $(X_j)_j$ and $(\breve W_j)_j$, respectively, and*
- *all conditions are replaced by corresponding conditions that hold uniformly in $j$,*

*then the results of Lemma 2.3 should be interpreted to hold uniformly in $j$.*

In the remainder of this section, we will apply Lemma 2.3, or precisely Remark 2.4, with $X_j = V_{j+1}$. Then Part (a) of Lemma 2.3, with $\breve{V}_j = V_j$, will be used to to verify the existence of the uniformly bounded biorthogonal projectors $Q_j$, and both parts of Lemma 2.3, with a generally different choice for $\breve{V}_j$, will be used to construct wavelet bases for the detail spaces $V_{j+1} \cap \tilde{V}_j^{\perp_{L^2}}$. For the special case that $\breve{V}_j = V_j$ in Part (b), in the literature the spaces $\breve{W}_j$ are known as *initial stable completions* ([CDP96]).

Aiming at improving the condition numbers of the wavelet bases from [DS99c], in the following proposition we study the statements of Lemma 2.3 quantitatively:

**Proposition 2.5.** *In the situation of Lemma 2.3, let*

$$\delta := \inf_{0 \neq \breve{v} \in \breve{V}} \sup_{0 \neq \tilde{v} \in \tilde{V}} \frac{|\langle \breve{v}, \tilde{v} \rangle|}{\|\breve{v}\| \|\tilde{v}\|} \quad \textit{and} \quad \epsilon := \cos \angle(\breve{W}, \breve{V}),$$

*then*

$$\|P\|_{L^2 \to L^2} = \delta^{-1} \quad \textit{and} \quad \|((I-P)_{|\breve{W}})^{-1}\|_{L^2 \to L^2} \leq (1-\epsilon)^{-\frac{1}{2}}.$$

*Proof:* On one hand, since $\operatorname{Im} P = \breve{V}$ and $\operatorname{Im}(I-P) = \tilde{V}^{\perp}$, for $x \in L^2$ we have

$$\|Px\| \leq \frac{1}{\delta} \sup_{0 \neq \tilde{v} \in \tilde{V}} \frac{|\langle Px, \tilde{v} \rangle|}{\|\tilde{v}\|} = \frac{1}{\delta} \sup_{0 \neq \tilde{v} \in \tilde{V}} \frac{|\langle x, \tilde{v} \rangle|}{\|\tilde{v}\|} \leq \frac{1}{\delta} \|x\|.$$

On the other hand, since for any $\breve{v} \in \breve{V}$, $\exists ! \tilde{u} \in \tilde{V}$ such that $P\tilde{u} = \breve{v}$, we have

$$\inf_{0 \neq \breve{v} \in \breve{V}} \sup_{0 \neq \tilde{v} \in \tilde{V}} \frac{|\langle \breve{v}, \tilde{v} \rangle|}{\|\breve{v}\| \|\tilde{v}\|} = \inf_{0 \neq \tilde{u} \in \tilde{V}} \sup_{0 \neq \tilde{v} \in \tilde{V}} \frac{|\langle P\tilde{u}, \tilde{v} \rangle|}{\|P\tilde{u}\| \|\tilde{v}\|} = \inf_{0 \neq \tilde{u} \in \tilde{V}} \sup_{0 \neq \tilde{v} \in \tilde{V}} \frac{|\langle \tilde{u}, \tilde{v} \rangle|}{\|P\tilde{u}\| \|\tilde{v}\|} = \inf_{0 \neq \tilde{u} \in \tilde{V}} \frac{\|\tilde{u}\|}{\|P\tilde{u}\|},$$

so that

$$\delta = \inf_{0 \neq \tilde{u} \in \tilde{V}} \frac{\|\tilde{u}\|}{\|P\tilde{u}\|} = \Big( \sup_{0 \neq \tilde{u} \in \tilde{V}} \frac{\|P\tilde{u}\|}{\|\tilde{u}\|} \Big)^{-1} \geq \Big( \sup_{0 \neq x \in L^2} \frac{\|Px\|}{\|x\|} \Big)^{-1} = \|P\|_{L^2 \to L^2}^{-1}.$$

Further, since for any $\psi \in X \cap \tilde{V}^{\perp}$, $\exists ! \xi \in \breve{W}$ such that $\psi = (I-P)\xi$, we have

$$\begin{aligned} \|\psi\|^2 &= \|\xi\|^2 + \|P\xi\|^2 - 2\langle \xi, P\xi \rangle \\ &\geq \|\xi\|^2 + \|P\xi\|^2 - \epsilon(\|\xi\|^2 + \|P\xi\|^2) \\ &\geq (1-\epsilon)\|\xi\|^2 \\ &= (1-\epsilon)\|((I-P)_{|\breve{W}})^{-1}\psi\|^2. \end{aligned}$$

□

As a consequence of Lemma 2.3 and Proposition 2.5, we obtain

**Corollary 2.6.** *Let $(V_j)_j$ and $(\tilde{V}_j)_j$ be two* sequences *of closed subspaces of $L^2$. Suppose that*

($\mathcal{A}1$) $\tilde{\Phi}_j$ *is an uniform Riesz basis for $\tilde{V}_j$, and*

($\mathcal{A}2$) $\Theta_j \cup \Xi_j$ *is an uniform Riesz basis for $V_{j+1}$ with $\langle \Theta_j, \tilde{\Phi}_j \rangle = Id$.*

*Then*

$$\Psi_j := \Xi_j - \langle \Xi_j, \tilde{\Phi}_j \rangle \Theta_j, \tag{2.1}$$

*whose elements are called* (biorthogonal) wavelets*, is an uniform Riesz basis for the space* $V_{j+1} \cap \tilde{V}_j^{\perp}$ *with*

$$\kappa_{\Psi_j} \leq \frac{(1+\delta_j^{-1})}{(1-\epsilon_j)^{\frac{1}{2}}} \kappa_{\Xi_j}, \tag{2.2}$$

*where*

$$\delta_j := \inf_{0 \neq z_j \in \operatorname{span} \Theta_j} \sup_{0 \neq \tilde{v}_j \in \tilde{V}_j} \frac{|\langle z_j, \tilde{v}_j \rangle|}{\|z_j\| \|\tilde{v}_j\|} > 0$$

*and*

$$\epsilon_j := \cos \angle(\operatorname{span} \Theta_j, \operatorname{span} \Xi_j) < 1.$$

*Proof:* We are going to apply Lemma 2.3, or precisely Remark 2.4, with $\breve{V}_j := \operatorname{span} \Theta_j$, $\breve{W}_j := \operatorname{span} \Xi_j$ and $X_j := V_{j+1}$ as follows: Note that, per definition, $\Theta_j$ is an uniform Riesz basis for $\breve{V}_j$. Further, since $\langle \Theta_j, \tilde{\Phi}_j \rangle = Id$, $(\breve{V}_j, \tilde{V}_j)$ satisfies the condition (i) in Lemma 2.3(a) uniformly in $j$. Hence, $\delta_j > 0$ and there exist (unique) uniformly bounded projector $P_j$ with $\operatorname{Im} P_j = \breve{V}_j$ and $\operatorname{Im}(I - P_j) = \tilde{V}_j^{\perp}$.

In addition, since $\Theta_j \cup \Xi_j$ is an uniform Riesz basis for $V_{j+1}$, $V_{j+1} = \breve{W}_j + \breve{V}_j$ and $\epsilon_j < 1$ uniformly in $j$. Hence, by Lemma 2.3(b), $(I - P_j)_{|\breve{W}_j} : \breve{W}_j \to V_{j+1} \cap \tilde{V}_j^{\perp}$ is uniformly boundedly invertible. This implies that the $(I - P_j)_{|\breve{W}_j}$ map uniform Riesz bases to uniform Riesz bases, i.e.,

$$\Psi_j := (I - P_j)\Xi_j \tag{2.3}$$

is an uniform Riesz basis for the space $V_{j+1} \cap \tilde{V}_j^{\perp}$. Since

$$P_j x = \langle x, \tilde{\Phi}_j \rangle \langle \Theta_j, \tilde{\Phi}_j \rangle^{-1} \Theta_j = \langle x, \tilde{\Phi}_j \rangle \Theta_j,$$

the wavelet formula (2.3) is equivalent to (2.1). Finally, by using the wavelet formula (2.3), we infer that, for all $\mathbf{c}_j \in l_2(\Psi_j) = l_2(\Xi_j)$,

$$\|((I - P_j)_{|\breve{W}_j})^{-1}\|_{L^2 \to L^2}^{-1} \|\mathbf{c}_j^T \Xi_j\| \leq \|\mathbf{c}_j^T \Psi_j\| \leq \|(I - P_j)_{|\breve{W}_j}\|_{L^2 \to L^2} \|\mathbf{c}_j^T \Xi_j\|,$$

and so, by using Proposition 2.5, we obtain

$$\kappa_{\Psi_j} \leq \frac{(1+\delta_j^{-1})}{(1-\epsilon_j)^{\frac{1}{2}}} \kappa_{\Xi_j},$$

which concludes the proof. □

**Remark 2.7.** *Note that the wavelet basis $\Psi_j$ constructed above depends on $V_{j+1}$, $\tilde{V}_j$, $\breve{V}_j$ and $\Xi_j$, but, as follows from (2.3), not on the choice of the bases $\Theta_j$ and $\tilde{\Phi}_j$ for $\breve{V}_j$ and $\tilde{V}_j$, respectively.*

Thus, in order to have uniform $L^2$-Riesz bases for $V_{j+1} \cap \tilde{V}_j^{\perp_{L^2}}$, the above corollary shows that it is sufficient to construct $L^2$-Riesz bases $\tilde{\Phi}_j$ for $\tilde{V}_j$ and $\Theta_j \cup \Xi_j$ for $V_{j+1}$ such that $\langle \Theta_j, \tilde{\Phi}_j \rangle_{L^2} = Id$. In this paper, we will consider $V_j$ and $\tilde{V}_j$ to be *Lagrange finite element spaces* with respect to a common triangulation. By adopting finite element techniques, this allows us to reduce the construction of such collections $\tilde{\Phi}_j$, $\Theta_j$ and $\Xi_j$ of *global* functions on the underlying domain to a construction of corresponding collections of *local* functions on a single reference element. Furthermore, we will derive an upper bound for the right hand side of (2.2) in terms of similar local quantities which, in particular, are independent of $j$.

2.3. **Reduction to a reference element.** Our reference element will be the following closed $n$-simplex:

$$\boldsymbol{T} = \{\lambda \in I\!R^{n+1} : \sum_{i=1}^{n+1} \lambda_i = 1, \lambda_i \geq 0\}.$$

We fix a refinement of $\boldsymbol{T}$ into $2^n$ congruent subsimplices $\boldsymbol{T}_1, \cdots, \boldsymbol{T}_{2^n}$, each of them determined by some ordered set of vertices.

For any closed $n$-simplex $T$, let $\lambda_T(x) \in \boldsymbol{T}$ denote the barycentric coordinates of $x \in T$ with respect to the set of vertices of $T$ equipped with some ordering. The above dyadic refinement of $\boldsymbol{T}$ induces such a refinement of $T$ into $2^n$ congruent subsimplices $(\lambda_T^{-1} \circ \lambda_{\boldsymbol{T}_k}^{-1} \circ \lambda_T)(T)$, $1 \leq k \leq 2^n$, see Figure 2 for an illustration.

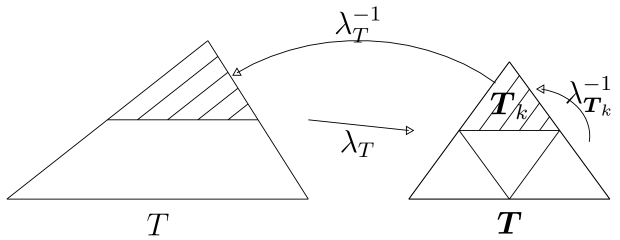


FIGURE 2. The induced dyadic refinement ($n = 2$).

Further, let $\tau_0$ be a fixed collection of closed $n$-simplices, or elements, such that $\cup_{T \in \tau_0} T$ is a partition, also referred to as *triangulation* or *mesh*, of the closure of some open domain $\Omega \subset I\!R^n$. We assume that the triangulation is conforming, i.e., the intersection of any two elements is either empty or a common face. Here with a face of $T$, we mean any closed $n'$-simplex spanned by $n' + 1$ vertices of $T$, where $0 \leq n' < n$. Starting from $\tau_0$, we obtain an infinite sequence of collections of simplices $(\tau_j)_{j \geq 0}$ by defining $\tau_{j+1}$ as the collection of all simplices that arise by applying above refinement to all simplices from $\tau_j$. So for any $j$, $\cup_{T \in \tau_j} T$ is a triangulation of $\overline{\Omega}$ generated by a $j$-times repeated dyadic refinement of the initial triangulation $\cup_{T \in \tau_0} T$. To avoid some technical complications, we will always assume that $n \leq 3$, meaning that automatically all these triangulations are conforming.

In the rest of this section, we will merely consider collections of continuous functions $\boldsymbol{\Sigma} = \{\boldsymbol{\sigma}_\lambda : \lambda \in \boldsymbol{I}\}$ on $\boldsymbol{T}$ with some index set $\boldsymbol{I} = \boldsymbol{I}_{\boldsymbol{\Sigma}} \subset \boldsymbol{T}$ that satisfy

($\mathcal{V}$) $\boldsymbol{\sigma}_\lambda$ vanishes on any face that does not include $\lambda$,
($\mathcal{S}$) $\pi(\boldsymbol{I}) = \boldsymbol{I}$ and $\boldsymbol{\sigma}_\lambda = \boldsymbol{\sigma}_{\pi(\lambda)} \circ \pi$ for any permutation $\pi : I\!R^{n+1} \to I\!R^{n+1}$,
($\mathcal{I}$) For $\boldsymbol{e} = \boldsymbol{T}$, or for $\boldsymbol{e}$ being any face of $\boldsymbol{T}$, $\{\boldsymbol{\sigma}_{\lambda|_{\boldsymbol{e}}} : \lambda \in \boldsymbol{I} \cap \boldsymbol{e}\}$ is independent.

Note that ($\mathcal{I}$) in particular implies that $\boldsymbol{\Sigma}$ is a collection of independent functions, so that $\boldsymbol{\Sigma}$ is an $L^2$-Riesz basis for its span.

Such collections of local functions can be used to assemble collections of global functions in a way known from finite element methods: For $j \geq 0$ and with

$$I_{\Sigma_j} := \{x \in \Omega : \lambda_T(x) \in \boldsymbol{I} \text{ for some } T \in \tau_j\}, \tag{2.4}$$

we define the collection $\Sigma_j = \{\sigma_{j,x} : x \in I_{\Sigma_j}\}$ of functions on $\Omega$ by

$$\sigma_{j,x}(y) = \begin{cases} \mu(x;\tau_j)\boldsymbol{\sigma}_{\lambda_T(x)}(\lambda_T(y)) & \text{if } x, y \in T \in \tau_j \\ 0 & \text{otherwise} \end{cases} \tag{2.5}$$

with the scaling factor $\mu(x;\tau_j) := \left(\sum_{\{T \in \tau_j : T \ni x\}} \frac{\mathrm{vol}(T)}{\mathrm{vol}(\boldsymbol{T})}\right)^{-\frac{1}{2}}$. Note that, the continuity of $\boldsymbol{\sigma}_\lambda$ and the assumptions ($\mathcal{V}$), ($\mathcal{S}$) and ($\mathcal{I}$) show that $\Sigma_j$ are collections of well-defined, continuous and independent functions on $\Omega$. An illustration of this assembling process is given in Figure 3.

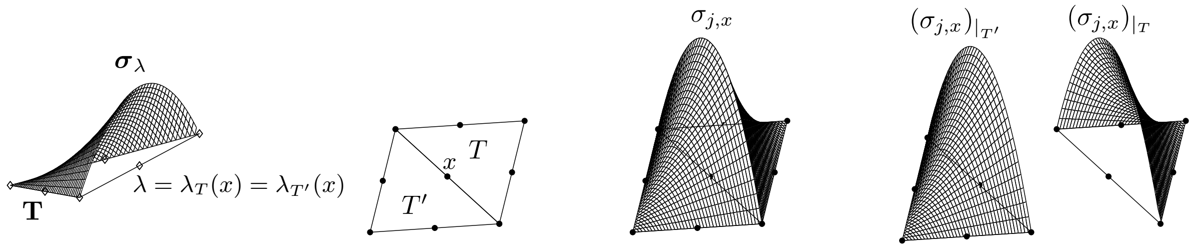


FIGURE 3. The nodal basis of the Lagrange finite element space of order 3 contains two types of basis functions. In this figure the assembling is illustrated of the bubble functions associated to the midpoints from functions of a basis $\boldsymbol{\Sigma}$ for $P_2(\mathbf{T})$ that satisfies ($\mathcal{V}$), ($\mathcal{S}$) and ($\mathcal{I}$).

We collect some results that will be used in our analysis (see [Ngu05, §3.2] for a proof):

**Lemma 2.8.** *Let $\boldsymbol{\Sigma}$ and $\tilde{\boldsymbol{\Sigma}}$ be two collections of 'local' functions (on $\boldsymbol{T}$) both satisfying ($\mathcal{V}$), ($\mathcal{S}$) and ($\mathcal{I}$). Let $\Sigma_j$ and $\tilde{\Sigma}_j$ denote the corresponding collections of 'global' functions (on $\Omega$). Then:*

(i) *The collections $\Sigma_j$ are uniform $L^2$-Riesz systems. In particular, $\lambda_{L^2(\Omega),\Sigma_j} \geq \lambda_{L^2(\boldsymbol{T}),\boldsymbol{\Sigma}}$ and $\Lambda_{L^2(\Omega),\Sigma_j} \leq \Lambda_{L^2(\boldsymbol{T}),\boldsymbol{\Sigma}}$, and so*

$$\kappa_{L^2(\Omega),\Sigma_j} \leq \kappa_{L^2(\boldsymbol{T}),\boldsymbol{\Sigma}}.$$

(ii) *If $\langle \boldsymbol{\Sigma}, \tilde{\boldsymbol{\Sigma}}\rangle_{L^2(\boldsymbol{T})} = \mathbf{Id}$, then $\langle \Sigma_j, \tilde{\Sigma}_j\rangle_{L^2(\Omega)} = Id$.*

(iii) *Suppose that $\boldsymbol{I}_{\boldsymbol{\Sigma}} = \boldsymbol{I}_{\tilde{\boldsymbol{\Sigma}}}$. Then*

$$\Re\langle \boldsymbol{\Sigma}, \tilde{\boldsymbol{\Sigma}}\rangle_{L^2(\boldsymbol{T})} \geq \lambda_{\Re} \Longrightarrow \Re\langle \Sigma_j, \tilde{\Sigma}_j\rangle_{L^2(\Omega)} \geq \lambda_{\Re}.$$

(iv) $\cos \angle_{L^2(\Omega)}(\operatorname{span} \Sigma_j, \operatorname{span} \tilde{\Sigma}_j) \leq \cos \angle_{L^2(\boldsymbol{T})}(\operatorname{span} \boldsymbol{\Sigma}, \operatorname{span} \tilde{\boldsymbol{\Sigma}})$.

(v) *Suppose* $\langle \boldsymbol{\Sigma}, \tilde{\boldsymbol{\Sigma}} \rangle_{L^2(\boldsymbol{T})} = \mathbf{Id}$. *Let*

$$\delta_j := \inf_{0 \neq u_j \in \operatorname{span} \Sigma_j} \sup_{0 \neq \tilde{u}_j \in \operatorname{span} \tilde{\Sigma}_j} \frac{|\langle u_j, \tilde{u}_j \rangle_{L^2(\Omega)}|}{\|u_j\|_{L^2(\Omega)} \|\tilde{u}_j\|_{L^2(\Omega)}}$$

*and*

$$\boldsymbol{\delta} := \inf_{0 \neq \mathbf{u} \in \operatorname{span} \boldsymbol{\Sigma}} \sup_{0 \neq \tilde{\mathbf{u}} \in \operatorname{span} \tilde{\boldsymbol{\Sigma}}} \frac{|\langle \mathbf{u}, \tilde{\mathbf{u}} \rangle_{L^2(\boldsymbol{T})}|}{\|\mathbf{u}\|_{L^2(\boldsymbol{T})} \|\tilde{\mathbf{u}}\|_{L^2(\boldsymbol{T})}}.$$

*Then*

$$\delta_j \geq \boldsymbol{\delta} \kappa_{\boldsymbol{\Sigma}}^{-\frac{1}{2}}.$$

2.4. **Definition of primal and dual spaces.** In the following, for $\check{d}, \check{p} \in I\!N_0$ and $T$ being any closed $n$-simplex, $P_{\check{d},\check{p}}(T)$ will denote the space of continuous piecewise polynomials on $T$ of degree $\check{d}$ with respect to a $\check{p}$-times repeated dyadic refinement of $T$. With $\boldsymbol{I}_\ell$ being the *principal lattice* of order $\ell$ defined by

$$\boldsymbol{I}_\ell = \{\lambda \in \boldsymbol{T} : \ell \lambda_i \in I\!N_0\},$$

it is well-known that

$$\dim(P_{\check{d},\check{p}}(\boldsymbol{T})) = \operatorname{card}(\boldsymbol{I}_{\check{d}2^{\check{p}}}).$$

Now, in view of the requirement $\tilde{d} + 2r > d$ when dealing with integral equations where $r$ might be negative (cf. [Sch98] and [Ngu05, §5.4]), we like to construct pairs of $\tilde{V}_j$ and $V_j$ satisfying Jackson estimates with general parameters $\tilde{d} \geq d$, respectively. Further, as one can readily verify (e.g., by using the equivalences stated in Lemma 2.3), $\dim(\tilde{V}_j) = \dim(V_j)$ is a necessary condition for the existence of the uniformly bounded projectors $Q_j : L^2 \to L^2$ with $\operatorname{Im} Q_j = V_j$ and $\operatorname{Im}(I - Q_j) = \tilde{V}_j^{\perp_{L^2}}$. In view of these considerations, we define $(V_j)_j$ and $(\tilde{V}_j)_j$ by

$$V_j = \{v \in C(\Omega) : v_{|T} \in P_{d-1,p}(T)\,,\, T \in \tau_j\} \tag{2.6}$$

and

$$\tilde{V}_j = \{\tilde{v} \in C(\Omega) : \tilde{v}_{|T} \in P_{\tilde{d}-1,0}(T)\,,\, T \in \tau_j\}, \tag{2.7}$$

where we restrict ourselves to $\tilde{d}$ and $d$ such that

$$(d-1)2^p = \tilde{d} - 1 \text{ for some } p \in I\!N_0. \tag{2.8}$$

Since

$$\dim(P_{\tilde{d}-1,0}(T)) = \dim(P_{d-1,p}(T)),$$

we indeed have $\dim(\tilde{V}_j) = \dim(V_j)$.

With this choice of $(V_j)_j$ and $(\tilde{V}_j)_j$, it is obvious that $V_j \subset V_{j+1}$ and $\tilde{V}_j \subset \tilde{V}_{j+1}$. Further, it is well-known that $(V_j)_j$ and $(\tilde{V}_j)_j$ satisfy the *Jackson estimates* with parameters $d$ and $\tilde{d}$ as well as the *Bernstein estimates* with parameters $\gamma = \tilde{\gamma} = \frac{3}{2}$ (see e.g., [Osw94, Dah97, Ste03]). In the remainder of this subsection, we will show how to verify the existence of the *uniformly bounded biorthogonal projectors* $Q_j : L^2 \to L^2$ with $\operatorname{Im} Q_j = V_j$ and $\operatorname{Im}(I - Q_j) = \tilde{V}_j^{\perp_{L^2}}$, being the remaining assumption made in Theorem 2.1.

To this end, let $\mathbf{\Phi} = \{\psi_\lambda : \lambda \in \mathbf{I}_{\mathbf{\Psi}}\}$ and $\tilde{\mathbf{\Phi}} = \{\tilde{\psi}_\lambda : \lambda \in \mathbf{I}_{\tilde{\mathbf{\Psi}}}\}$ be two collections of continuous functions on $\boldsymbol{T}$ satisfying ($\mathcal{V}$), ($\mathcal{S}$) and ($\mathcal{I}$) with

$$\boldsymbol{I}_{\mathbf{\Phi}} = \boldsymbol{I}_{\tilde{\mathbf{\Phi}}} = \boldsymbol{I}_{\tilde{d}-1},$$

$$\operatorname{span} \mathbf{\Phi} = P_{d-1,p}(\boldsymbol{T}), \tag{2.9}$$

and

$$\operatorname{span} \tilde{\mathbf{\Phi}} = P_{\tilde{d}-1,0}(\boldsymbol{T}). \tag{2.10}$$

Note that, with

$$I_j := I_{\Phi_j} = I_{\tilde{\Phi}_j}$$

being the global index set corresponding to $\boldsymbol{I}_{\tilde{d}-1}$ defined according to (2.4), it is well-known that

$$\operatorname{card}(I_j) = \dim(V_j),$$

so that $\operatorname{card}(\Phi_j) = \operatorname{card}(I_j) = \dim(V_j)$. Thus, since $\Phi_j \subset V_j$ and the elements of $\Phi_j$ are independent functions, $\Phi_j$ is a basis for $V_j$. What is more, by Lemma 2.8(i), the $\Phi_j$ are *uniform $L^2$-Riesz bases for $V_j$*. Analogously, with $\tilde{\Phi}_j$ being the collection of global functions corresponding to $\tilde{\mathbf{\Phi}}$, the $\tilde{\Phi}_j$ are *uniform $L^2$-Riesz bases for $\tilde{V}_j$*.

**Proposition 2.9.** *Consider $V_j$, $\tilde{V}_j$, $\mathbf{\Phi}$ and $\tilde{\mathbf{\Phi}}$ given above. If*

$$\Re\langle \mathbf{\Phi}, \tilde{\mathbf{\Phi}} \rangle_{L^2(\boldsymbol{T})} > 0, \tag{2.11}$$

*then there exist uniformly bounded biorthogonal projectors $Q_j : L^2 \to L^2$ with $\operatorname{Im} Q_j = V_j$ and $\operatorname{Im}(I - Q_j) = \tilde{V}_j^{\perp_{L^2}}$.*

*Proof:* As mentioned before, the collections of global functions $\Phi_j$ and $\tilde{\Phi}_j$ given above are uniform $L^2$-Riesz bases for $V_j$ and $\tilde{V}_j$, respectively. From part (a) of Lemma 2.3, or precisely Remark 2.4, with $(\breve{V}_j, \tilde{V}_j, H) = (V_j, \tilde{V}_j, L^2(\Omega))$, we learn that the existence of such $Q_j$ is then proven if the $\Re\langle \Phi_j, \tilde{\Phi}_j \rangle_{L^2}$ are uniformly positive definite. The latter simply follows from our assumption and Lemma 2.8(iii). $\square$

We apply the above proposition as follows. Consider the following *nodal* collections: For $\check{d}, \check{p} \in \mathbb{N}_0$, let

$$\mathbf{\Delta}^{(\check{d},\check{p})} = \{\boldsymbol{\delta}_\lambda^{(\check{d},\check{p})} : \lambda \in \boldsymbol{I}_{\check{d}2^{\check{p}}}\} \subset P_{\check{d},\check{p}}(\boldsymbol{T}) \tag{2.12}$$

be defined by

$$\boldsymbol{\delta}_\lambda^{(\check{d},\check{p})}(\mu) := \begin{cases} 1 & \lambda = \mu, \\ 0 & \lambda \neq \mu \in \boldsymbol{I}_{\check{d}2^{\check{p}}}. \end{cases}$$

Then $\mathbf{\Delta}^{(\check{d},\check{p})}$ satisfies $(\mathcal{V})$, $(\mathcal{S})$ and $(\mathcal{I})$ and spans $P_{\check{d},\check{p}}(\boldsymbol{T})$. In all concrete realizations in the next section (Section 3), we have verified the positive definiteness of $\Re\langle \mathbf{\Delta}^{(d-1,p)}, \mathbf{\Delta}^{(\tilde{d}-1,0)}\rangle_{L^2(\boldsymbol{T})}$, with which the existence of the uniformly bounded projectors $Q_j$ mentioned above is verified.

2.5. **A wavelet basis and a bound for its condition number.** With the spaces $V_j$ and $\tilde{V}_j$ and the collections $\tilde{\mathbf{\Phi}}$ and $\tilde{\Phi}_j$ defined above, in this subsection we will show how to construct uniform $L^2$-Riesz basis $\Theta_j \cup \Xi_j$ for $V_{j+1}$ such that $\langle \Theta_j, \tilde{\Phi}_j\rangle_{L^2} = Id$. For the resulting wavelets basis $\Psi_j$ constructed accordingly to Corollary 2.6, we derive an upper bound for $\kappa_{\Psi_j}$ involving local quantities only, which will guide us to make suitable choices in the wavelet realization described in the next section.

Let $\mathbf{\Theta}$ and $\mathbf{\Xi}$ be two collections of continuous functions on $\boldsymbol{T}$ both satisfying $(\mathcal{V})$, $(\mathcal{S})$ and $(\mathcal{I})$ with

$$\boldsymbol{I}_{\mathbf{\Theta}} = \boldsymbol{I}_{\tilde{\mathbf{\Phi}}} = \boldsymbol{I}_{\tilde{d}-1} \text{ and } \boldsymbol{I}_{\mathbf{\Xi}} = \boldsymbol{I}_{2(\tilde{d}-1)} \setminus \boldsymbol{I}_{\tilde{d}-1},$$

such that

$$\operatorname{span}\{\mathbf{\Theta} \cup \mathbf{\Xi}\} = P_{d-1,p+1}(\boldsymbol{T}) \tag{2.13}$$

and

$$\langle \mathbf{\Theta}, \tilde{\mathbf{\Phi}}\rangle_{L^2(\boldsymbol{T})} = \mathbf{Id}. \tag{2.14}$$

Note that the collection $\mathbf{\Theta} \cup \mathbf{\Xi}$ satisfies $(\mathcal{V})$, $(\mathcal{S})$ and, by (2.13), also $(\mathcal{I})$. Further, by construction it holds that $\Theta_j \cup \Xi_j \subset V_{j+1}$ and $\operatorname{card}(I_{\Theta_j \cup \Xi_j}) = \operatorname{card}(I_{j+1}) = \dim(V_{j+1})$, and so, since the elements of $\Theta_j \cup \Xi_j$ are independent functions, $\Theta_j \cup \Xi_j$ is a basis for $V_{j+1}$. What is more, by Lemma 2.8(i), the $\Theta_j \cup \Xi_j$ are *uniform $L^2$-Riesz bases for $V_{j+1}$*.

**Proposition 2.10.** *Consider $V_j$, $\tilde{V}_j$, $\tilde{\mathbf{\Phi}}$, $\mathbf{\Theta}$, $\mathbf{\Xi}$, $\tilde{\Phi}_j$, $\Theta_j$ and $\Xi_j$ as given above. Let*

$$\boldsymbol{\delta} := \inf_{0\neq \mathbf{z}\in \operatorname{span}\mathbf{\Theta}} \sup_{0\neq \tilde{\mathbf{v}}\in \operatorname{span}\tilde{\mathbf{\Phi}}} \frac{|\langle \mathbf{z}, \tilde{\mathbf{v}}\rangle_{L^2(\boldsymbol{T})}|}{\|\mathbf{z}\|_{L^2(\boldsymbol{T})}\|\tilde{\mathbf{v}}\|_{L^2(\boldsymbol{T})}},$$

$$\boldsymbol{\epsilon} := \cos\angle_{L^2(\boldsymbol{T})}(\operatorname{span}\mathbf{\Theta}, \operatorname{span}\mathbf{\Xi}).$$

*Then*

$$\Psi_j := \Xi_j - \langle \Xi_j, \tilde{\Phi}_j\rangle_{L^2(\Omega)}\Theta_j \tag{2.15}$$

*is an uniform $L^2$-Riesz basis for $V_{j+1} \cap \tilde{V}_j^{\perp_{L^2(\Omega)}}$, and*

$$\kappa_{L^2(\Omega),\Psi_j} \leq \frac{1 + \boldsymbol{\delta}^{-1}\kappa^{\frac{1}{2}}_{L^2(\boldsymbol{T}),\tilde{\mathbf{\Phi}}}}{(1-\boldsymbol{\epsilon})^{\frac{1}{2}}}\kappa_{L^2(\boldsymbol{T}),\mathbf{\Xi}}. \tag{2.16}$$

*Proof:* As mentioned before, the collections of global functions $\tilde{\Phi}_j$ and $\Theta_j \cup \Xi_j$ given above are uniform $L^2$-Riesz bases for $\tilde{V}_j$ and $V_{j+1}$, respectively. Further, by Lemma 2.8(ii), the biorthogonality between $\mathbf{\Theta}$ and $\tilde{\mathbf{\Phi}}$ in (2.14) implies the biorthogonality between $\Theta_j$ and $\tilde{\Phi}_j$, i.e., $\langle \Theta_j, \tilde{\Phi}_j\rangle_{L^2(\Omega)} = Id$.

Thus, the two assumptions ($\mathcal{A}1$) and ($\mathcal{A}2$) made in Corollary 2.6 are satisfied. With

$$\delta_j := \inf_{0\neq z_j\in \operatorname{span}\Theta_j} \sup_{0\neq \tilde{v}_j\in\tilde{V}_j} \frac{|\langle z_j, \tilde{v}_j\rangle_{L^2(\Omega)}|}{\|z_j\|_{L^2(\Omega)}\|\tilde{v}_j\|_{L^2(\Omega)}} > 0$$

and

$$\epsilon_j := \cos\angle_{L^2(\Omega)}(\operatorname{span}\Theta_j, \operatorname{span}\Xi_j) < 1,$$

it follows from Corollary 2.6 that

$$\kappa_{L^2(\Omega),\Psi_j} \leq \frac{(1+\delta_j^{-1})}{(1-\epsilon_j)^{\frac{1}{2}}}\kappa_{L^2(\Omega),\Xi_j}.$$

In addition, we learn from Lemma 2.8(i), (iv) and (v) that $\kappa_{L^2(\Omega),\Xi_j} \leq \kappa_{L^2(\boldsymbol{T}),\boldsymbol{\Xi}}$, $\epsilon_j \leq \boldsymbol{\epsilon}$ and $\delta_j \geq \boldsymbol{\delta}\kappa_{\boldsymbol{\Sigma}}^{-\frac{1}{2}}$, hence

$$\kappa_{L^2(\Omega),\Psi_j} \leq \frac{1+\boldsymbol{\delta}^{-1}\kappa^{\frac{1}{2}}_{L^2(\boldsymbol{T}),\tilde{\boldsymbol{\Phi}}}}{(1-\boldsymbol{\epsilon})^{\frac{1}{2}}}\kappa_{L^2(\boldsymbol{T}),\boldsymbol{\Xi}},$$

which concludes the proof. □

Note that, by construction, $\Psi_j = \{\psi_{j,x} : x \in I_{\Psi_j}\}$ where $I_{\Psi_j} = I_{\Xi_j} = I_{j+1} \setminus I_j$. Further, given $\Omega$ equipped with some initial triangulation $\tau_0$, and $d$ and $\tilde{d}$, the multiresolution analyses $(V_j)_j$ and $(\tilde{V}_j)_j$ are now uniquely determined. In the next section, dealing with concrete realizations, we will employ the remaining freedom in the wavelet construction to minimize the right hand side of (2.16). We conclude this section by collecting some attractive properties of our locally supported biorthogonal wavelets:
**Riesz bases properties:** From Subsection 2.4, we learn that the sequences of primal and dual spaces $(V_j)_j$ and $(\tilde{V}_j)_j$ satisfy the *Jackson estimates* with parameters $d$ and $\tilde{d}$ as well as the *Bernstein estimates* with parameters $\gamma = \tilde{\gamma} = \frac{3}{2}$, respectively. As mentioned at the end of Subsect. 2.4 we have verified the existence of the uniformly bounded biorthogonal projectors $Q_j$ in various concrete cases. Hence, in such cases, Theorem 2.1 and Corollary 2.2 guarantee that, for $s \in (-\frac{3}{2}, \frac{3}{2})$, the collection $\cup_{j=-1}^{\infty} 2^{-js}\Psi_j$ is a Riesz basis for $H^s$.
**Cancellation properties:** In addition, since $\psi_{j,x} \perp_{L^2} \tilde{V}_j$ and $\operatorname{diam}(\operatorname{supp}\psi_{j,x}) \lesssim 2^{-j}$, the wavelets $\psi_{j,x}$ have the so-called *cancellation property of order* $\tilde{d}$, meaning that, for any $p \in [1,\infty]$ and all smooth functions $f$ on $\Omega$, we have (cf. [Ste03, Ste04])

$$|\langle f, \psi_{j,x}\rangle_{L^2}| \lesssim 2^{-(\tilde{d}+\frac{n}{2}-\frac{n}{p})j}|f|_{W_p^{\tilde{d}}(\operatorname{supp}\psi_{j,x})}.$$

**Remark 2.11.** *As mentioned in* [Ste03], *with $\partial\Omega_D$ being either $\partial\Omega$ or a part of it consisting of the union of some $(n-1)$ dimensional faces of $T \in \tau_0$, homogeneous Dirichlet conditions on $\partial\Omega_D$ can simply be incorporated in our construction as follows: For $x$ being on $\partial\Omega_D$, the corresponding $\tilde{\phi}_{j,x}$, $\theta_{j,x}$ and $\xi_{j,x}$ are excluded from $\tilde{\Phi}_j$, $\Theta_j$ and $\Xi_j$. The resulting spaces $V_j$, $\tilde{V}_j$ are the standard Lagrange finite element spaces in which these boundary conditions* *are incorporated, and the two resulting multiresolution analyses* $(V_j)_j$, $(\tilde{V}_j)_j$ *satisfy all assumptions made in Theorem 2.1 with the same parameters* $d$, $\gamma$, $\tilde{d}$ *and* $\tilde{\gamma}$ *as in the case of 'full' spaces, where now the 'full' spaces* $H^s = H^s(\Omega)$ *should be replaced by*

$$\mathcal{H}^s := \begin{cases} H^s_{0,\partial\Omega_D}(\Omega) & \text{if } s \in [0,1] \\ H^1_{0,\partial\Omega_D}(\Omega) \cap H^s(\Omega) & \text{if } s > 1 \end{cases}$$

*and* $\mathcal{H}^s := (\mathcal{H}^{-s})'$ *if* $s < 0$. *Hence, the resulting* $\Psi_j$ *are uniform* $L^2$*-Riesz bases for the resulting* $V_{j+1} \cap \tilde{V}_j^{\perp_{L^2(\Omega)}}$ *and* $\cup_{j=-1}^{\infty} 2^{-js}\Psi_j$ *are Riesz bases for* $\mathcal{H}^s$ *for the same range of* $s$ *as in the case of 'full' spaces.*

*Note, however, that because of the boundary conditions imposed at the dual side, those* $\psi_{j,x}$ *having supports that extend to some* $T \in \tau_j$ *with a non-empty intersection with* $\partial\Omega_D$*, generally do not have any cancellation properties.*

## 3. Concrete realizations

In this section, we will drop the subscript $L^2$ where possible, i.e., we will write $\langle \cdot, \cdot \rangle$ for $\langle \cdot, \cdot \rangle_{L^2}$ etc.. Further, for $\mathcal{A}$ and $\tilde{\mathcal{A}}$ being subspaces of $L^2$, $P_{\mathcal{A}}(\cdot)$ will denote the $L^2$-orthogonal projection from $L^2$ onto $\mathcal{A}$ and $P_{\mathcal{A}}\tilde{\mathcal{A}} := \{P_{\mathcal{A}}\tilde{f} : \tilde{f} \in \tilde{\mathcal{A}}\} \subset \mathcal{A}$. Analogously, for $\Sigma$ being a collection of $L^2$ functions, $P_{\mathcal{A}}\Sigma := \{P_{\mathcal{A}}\sigma \ : \sigma \in \Sigma\}$.

First, recall Proposition 2.10 from the previous section: Let $\tilde{\mathbf{\Phi}}$, $\mathbf{\Theta}$ and $\Xi$ be three collections of continuous functions on $\boldsymbol{T}$ with index sets $\boldsymbol{I}_{\tilde{\mathbf{\Phi}}} = \boldsymbol{I}_{\mathbf{\Theta}} = \boldsymbol{I}_{\tilde{d}-1}$ and $\boldsymbol{I}_{\mathbf{\Xi}} = \boldsymbol{I}_{2(\tilde{d}-1)} \setminus \boldsymbol{I}_{\tilde{d}-1}$, satisfying $(\mathcal{V})$, $(\mathcal{S})$ and $(\mathcal{I})$ such that

- $\operatorname{span} \tilde{\mathbf{\Phi}} = P_{\tilde{d}-1,0}(\boldsymbol{T})$, and
- $\operatorname{span} \{\mathbf{\Theta} \cup \mathbf{\Xi}\} = P_{d-1,p+1}(\boldsymbol{T})$ with $\langle \mathbf{\Theta}, \tilde{\mathbf{\Phi}} \rangle = \mathbf{I}$.

Then, with $\tilde{\Phi}_j$, $\Theta_j$ and $\Xi_j$ being the corresponding collections of global functions on $\Omega$ assembled according to (2.5) and $\Psi_j = \Xi_j - \langle \Xi_j, \tilde{\Phi}_j \rangle_{L^2(\Omega)} \Theta_j$ being the wavelet bases for the detail spaces, we have

$$\kappa_{\Psi_j} \leq \frac{1 + \boldsymbol{\delta}^{-1} \kappa_{\tilde{\mathbf{\Phi}}}^{\frac{1}{2}}}{(1 - \boldsymbol{\epsilon})^{\frac{1}{2}}} \kappa_{\mathbf{\Xi}}, \tag{3.1}$$

with $\boldsymbol{\delta}$ and $\boldsymbol{\epsilon}$ being defined in Proposition 2.10, i.e., $\boldsymbol{\delta} = \inf_{0 \neq \mathbf{z} \in \operatorname{span} \mathbf{\Theta}} \cos \angle_{L^2(\boldsymbol{T})}(\mathbf{z}, \operatorname{span} \mathbf{\Xi})$ and $\boldsymbol{\epsilon} = \cos \angle_{L^2(\boldsymbol{T})}(\operatorname{span} \mathbf{\Theta}, \operatorname{span} \mathbf{\Xi})$.

In this section, we will construct $\tilde{\mathbf{\Phi}}$, $\mathbf{\Theta}$ and $\mathbf{\Xi}$ for several concrete values of $(n, d, \tilde{d})$. It turns out that, except for $d = \tilde{d} = 2$, we have some freedom in the construction of $\tilde{\mathbf{\Phi}}$, $\mathbf{\Theta}$ and $\mathbf{\Xi}$. In [DS99c] this freedom has been used to minimize the number of non-zero entries in $\langle \mathbf{\Xi}, \tilde{\mathbf{\Phi}} \rangle_{L^2(\boldsymbol{T})}$, and with that to minimize the supports of the resulting wavelets. Guided by the upper bound (3.1), we will use this freedom to construct $\tilde{\mathbf{\Phi}}$, $\mathbf{\Theta}$ and $\mathbf{\Xi}$ such that

- $\boldsymbol{\delta}$ is large
- $\boldsymbol{\epsilon}$, $\kappa_{\tilde{\mathbf{\Phi}}}$ and $\kappa_{\mathbf{\Xi}}$ are small.

In our realization below, we will simultaneously construct $\tilde{\mathbf{\Phi}}$ and $\mathbf{\Theta}$ aiming at making $\boldsymbol{\delta}$ large and $\kappa_{\tilde{\mathbf{\Phi}}}$ small. After that, we will construct $\Xi$ aiming at making both $\boldsymbol{\epsilon}$ and $\kappa_{\Xi}$ small.

3.1. **The case** $(d,\tilde{d})=(2,2)$**.** One may verify that, for $n\in\{1,2,3\}$, the only possible choice of $\tilde{\mathbf{\Phi}}$, $\mathbf{\Theta}$ and $\Xi$, up to an irrelevant scaling, is the one given in [DS99c]:

$$\tilde{\mathbf{\Phi}}=\mathbf{\Delta}^{(1,0)},$$

$$\boldsymbol{\theta}_\lambda=\frac{1}{\mathrm{vol}(\boldsymbol{T})}\,2^{(n+1)}(n+1)\left(\boldsymbol{\delta}_\lambda^{(1,1)}-2^{-(n+1)}\boldsymbol{\delta}_\lambda^{(1,0)}\right)\qquad(\lambda\in\boldsymbol{I}_1)$$

and

$$\boldsymbol{\xi}_\lambda=\boldsymbol{\delta}_\lambda^{(1,1)}\qquad(\lambda\in\boldsymbol{I}_2\setminus\boldsymbol{I}_1).$$

The collections $\tilde{\mathbf{\Phi}}$, $\mathbf{\Theta}$ and $\Xi$ for $n=2$ are illustrated in Figure 4.

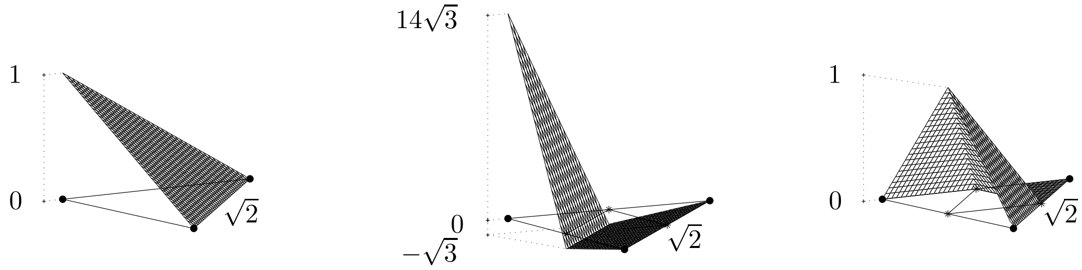


FIGURE 4. $\tilde{\boldsymbol{\phi}}\in\tilde{\mathbf{\Phi}}$ (left), $\boldsymbol{\theta}\in\mathbf{\Theta}$ (middle) and $\boldsymbol{\xi}\in\Xi$ (right) ($\{\bullet\}=\mathbf{I}_1$, $\{\times\}=\mathbf{I}_2\setminus\mathbf{I}_1$), $(n,d,\tilde{d})=(2,2,2)$

.

3.2. **The case** $(n,d,\tilde{d})=(1,2,3)$**.** In order to easily formulate the conditions $(\mathcal{V})$ and $(\mathcal{S})$, we have used $\boldsymbol{I}_{\tilde{d}-1}=\boldsymbol{I}_2$ and $\boldsymbol{I}_{2(\tilde{d}-1)}=\boldsymbol{I}_4$ as index sets for $\tilde{\mathbf{\Phi}}$ and $\mathbf{\Theta}\cup\Xi$, respectively. Yet, to view $\tilde{\mathbf{\Phi}}$, $\mathbf{\Theta}$ and $\Xi$ as vectors, the index sets $\{1,2,\cdots,\mathrm{card}\,\boldsymbol{I}_2\}$ and $\{1,2,\cdots,\mathrm{card}\,\boldsymbol{I}_4\}$ would be more appropriate. Therefore, we fix a numbering of $\boldsymbol{I}_2$ and $\boldsymbol{I}_4$ as in Figure 5, so that we can switch between these numbers and the corresponding barycentric coordinates at our convenience. Further, $\mathbf{\Delta}^{(1,2)}$ and $\mathbf{\Delta}^{(2,0)}$, with their elements being indexed according to the given numbering, are illustrated in Figure 6.

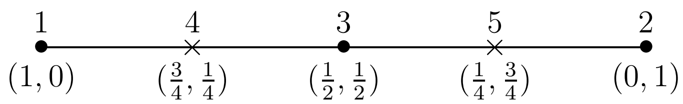


FIGURE 5. Numbering of $\boldsymbol{I}_2$ and $\boldsymbol{I}_4$ ($\bullet\in\boldsymbol{I}_2$, $\times\in\boldsymbol{I}_4\setminus\boldsymbol{I}_2$), $(n,d,\tilde{d})=(1,2,3)$.

In the realization below, the following aspects will be taken into account: It must hold that $\langle\mathbf{\Theta},\tilde{\mathbf{\Phi}}\rangle=\mathbf{I}$ with $\mathbf{\Theta}$ and $\tilde{\mathbf{\Phi}}$ satisfying $(\mathcal{S})$, $(\mathcal{I})$ and $(\mathcal{V})$. The last condition implies for

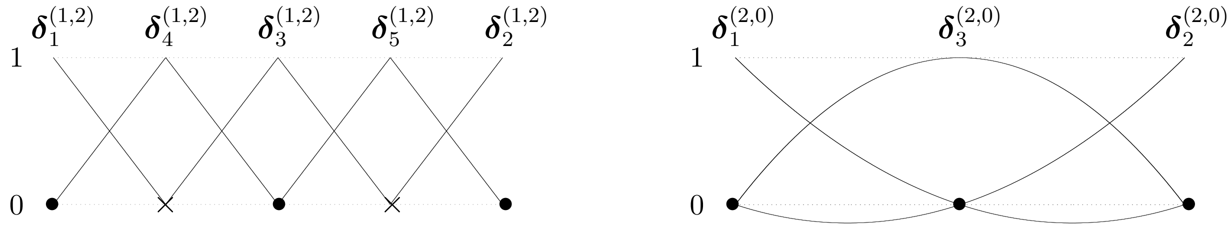


FIGURE 6. $\boldsymbol{\Delta}^{(1,2)}$ and $\boldsymbol{\Delta}^{(2,0)}$, $(n, d, \tilde{d}) = (1, 2, 3)$.

example that $\boldsymbol{\theta}_3$ and $\tilde{\boldsymbol{\phi}}_1$ must be elements of $\operatorname{span}\{\boldsymbol{\delta}_i^{(1,2)}\}_{i=3,4,5}$ and $\operatorname{span}\{\boldsymbol{\delta}_i^{(2,0)}\}_{i=1,3}$, respectively. In addition, any remaining freedom will be used to 'optimize' the four quantities $\boldsymbol{\delta}$, $\boldsymbol{\epsilon}$, $\kappa_{\tilde{\boldsymbol{\Phi}}}$ and $\kappa_{\boldsymbol{\Xi}}$. First, we construct the pair $(\tilde{\boldsymbol{\Phi}}, \boldsymbol{\Theta})$:

Step 1: In view of $(\mathcal{V})$, the only possible choice for $\tilde{\boldsymbol{\phi}}_3$ is $\tilde{\boldsymbol{\phi}}_3 = \boldsymbol{\delta}_3^{(2,0)}$. In order to make $\boldsymbol{\delta}$ large, we let $\mathcal{A}_3 := \operatorname{span}\{\boldsymbol{\delta}_i^{(1,2)}\}_{i=3,4,5}$ and take

$$\boldsymbol{\theta}_3 = \frac{1}{\langle P_{\mathcal{A}_3}\tilde{\boldsymbol{\phi}}_3, \tilde{\boldsymbol{\phi}}_3\rangle} P_{\mathcal{A}_3}\tilde{\boldsymbol{\phi}}_3.$$

Note that $\langle \tilde{\boldsymbol{\phi}}_3, \boldsymbol{\theta}_3\rangle = 1$.

Step 2: Next, we take

$$\tilde{\boldsymbol{\phi}}_1 = \boldsymbol{\delta}_1^{(2,0)} - \langle \boldsymbol{\delta}_1^{(2,0)}, \boldsymbol{\theta}_3\rangle \tilde{\boldsymbol{\phi}}_3.$$

$\tilde{\boldsymbol{\phi}}_2$ is obtained from $\tilde{\boldsymbol{\phi}}_1$ by permuting the barycentric coordinates. It holds in addition that $\langle \tilde{\boldsymbol{\phi}}_1, \boldsymbol{\theta}_3\rangle = \langle \tilde{\boldsymbol{\phi}}_2, \boldsymbol{\theta}_3\rangle = 0$.

Step 3: With the above $\tilde{\boldsymbol{\Phi}}$, again in order to make $\boldsymbol{\delta}$ large, we let $\mathcal{A}_1 := (\operatorname{span}\{\tilde{\boldsymbol{\phi}}_i\}_{i=2,3})^\perp \cap \operatorname{span}\{\boldsymbol{\delta}_i^{(1,2)}\}_{i=1,3,4,5}$ and take

$$\boldsymbol{\theta}_1 = \frac{1}{\langle P_{\mathcal{A}_1}\tilde{\boldsymbol{\phi}}_1, \tilde{\boldsymbol{\phi}}_1\rangle} P_{\mathcal{A}_1}\tilde{\boldsymbol{\phi}}_1.$$

$\boldsymbol{\theta}_2$ is obtained from $\boldsymbol{\theta}_1$ by permuting the barycentric coordinates.

By evaluating the above expressions, we find the coefficients of $\tilde{\boldsymbol{\Phi}}$ and $\boldsymbol{\Theta}$ with respect to $\boldsymbol{\Delta}^{(2,0)}$ and $\boldsymbol{\Delta}^{(1,2)}$ respectively. These coefficients are collected in the appendix. Next, we use $\boldsymbol{\Theta}$ to construct $\boldsymbol{\Xi}$:

Step 4: In order to make $\boldsymbol{\epsilon}$ small, we take

$$\operatorname{span}\boldsymbol{\Xi} = P_{\mathcal{A}_3}((\operatorname{span}\boldsymbol{\Theta})^\perp \cap P_{1,2}(\boldsymbol{T}))$$

with $\mathcal{A}_3$ being defined in step 1.

Step 5: In order to minimize $\kappa_{\boldsymbol{\Xi}}$, we are going to find an orthonormal basis for $\operatorname{span}\boldsymbol{\Xi}$ as follows: Let $\boldsymbol{\Theta}^\perp$ be a basis for $(\operatorname{span}\boldsymbol{\Theta})^\perp \cap P_{1,2}(\boldsymbol{T})$ satisfying $(\mathcal{S})$, then a basis $\boldsymbol{\Xi}^{(0)}$ for $\operatorname{span}\boldsymbol{\Xi}$ satisfying $(\mathcal{S})$ is given by

$$\boldsymbol{\Xi}^{(0)} = \begin{pmatrix} \boldsymbol{\xi}_4^{(0)} \\ \boldsymbol{\xi}_5^{(0)} \end{pmatrix} = P_{\mathcal{A}_3}\boldsymbol{\Theta}^\perp.$$

Now we take

$$\Xi = \langle \Xi^{(0)}, \Xi^{(0)} \rangle^{-\frac{1}{2}} \Xi^{(0)},$$

then $\Xi$ is an orthonormal basis for span $\Xi$ satisfying all three conditions ($\mathcal{V}$), ($\mathcal{S}$) and ($\mathcal{I}$). Further, it holds that span $\{\boldsymbol{\Theta} \cup \Xi\} = P_{1,2}(\boldsymbol{T})$. The coefficients of $\Xi$ with respect to $\boldsymbol{\Delta}^{(1,2)}$ are collected in the appendix.

3.3. **The case** $(n, d, \tilde{d}) = (2, 2, 3)$**.** In this case, we number the index sets $\boldsymbol{I}_{\tilde{d}-1} = \boldsymbol{I}_2$ and $\boldsymbol{I}_{2(\tilde{d}-1)} = \boldsymbol{I}_4$ as in Figure 7, and switch between these numbers and the corresponding barycentric coordinates at our convenience.

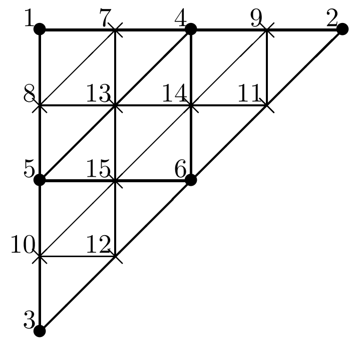


FIGURE 7. Numbering of $\boldsymbol{I}_2$ and $\boldsymbol{I}_4$ ($\bullet \in \boldsymbol{I}_2$, $\times \in \boldsymbol{I}_4 \setminus \boldsymbol{I}_2$), $(n, d, \tilde{d}) = (2, 2, 3)$

The realization below is carried out analogously to the one in the previous case:

Step 1: In view of ($\mathcal{V}$), the only possible choice for $\tilde{\boldsymbol{\phi}}_i$ for $i = 4, 5, 6$ is $\tilde{\boldsymbol{\phi}}_i = \boldsymbol{\delta}_i^{(2,0)}$. Also in view of ($\mathcal{V}$), span $\{\tilde{\boldsymbol{\phi}}_i\}_{i=1,4,5}$ has to be equal to span $\{\boldsymbol{\delta}_i^{(2,0)}\}_{i=1,4,5}$. We let $\mathcal{A}_6 :=$ (span $\{\boldsymbol{\delta}_i^{(2,0)}\}_{i=1,4,5})^\perp \cap$ span $\{\boldsymbol{\delta}_i^{(1,2)}\}_{i=6,11,12,13,14,15}$ and in order to make $\boldsymbol{\delta}$ large, we take

$$\boldsymbol{\theta}_6 = \frac{1}{\langle P_{\mathcal{A}_6} \tilde{\boldsymbol{\phi}}_6, \tilde{\boldsymbol{\phi}}_6 \rangle} P_{\mathcal{A}_6} \tilde{\boldsymbol{\phi}}_6.$$

Note that $\langle \tilde{\boldsymbol{\phi}}_4, \boldsymbol{\theta}_6 \rangle = \langle \tilde{\boldsymbol{\phi}}_5, \boldsymbol{\theta}_6 \rangle = 0$ whereas $\langle \tilde{\boldsymbol{\phi}}_6, \boldsymbol{\theta}_6 \rangle = 1$. $\boldsymbol{\theta}_4$ and $\boldsymbol{\theta}_5$ are obtained from $\boldsymbol{\theta}_6$ by permuting the barycentric coordinates.

Step 2: Next, we take

$$\tilde{\boldsymbol{\phi}}_1 = \boldsymbol{\delta}_1^{(2,0)} - \langle \boldsymbol{\delta}_1^{(2,0)}, \boldsymbol{\theta}_4 \rangle \tilde{\boldsymbol{\phi}}_4 - \langle \boldsymbol{\delta}_1^{(2,0)}, \boldsymbol{\theta}_5 \rangle \tilde{\boldsymbol{\phi}}_5.$$

$\tilde{\boldsymbol{\phi}}_2$ and $\tilde{\boldsymbol{\phi}}_3$ are obtained from $\tilde{\boldsymbol{\phi}}_1$ by permuting the barycentric coordinates. It holds in addition that $\langle \tilde{\boldsymbol{\phi}}_1, \boldsymbol{\theta}_6 \rangle = \langle \tilde{\boldsymbol{\phi}}_2, \boldsymbol{\theta}_6 \rangle = \langle \tilde{\boldsymbol{\phi}}_3, \boldsymbol{\theta}_6 \rangle = 0$.

Step 3: With the above $\tilde{\boldsymbol{\Phi}}$, we let $\mathcal{A}_1 :=$ (span $\{\tilde{\boldsymbol{\phi}}_i\}_{i=2,3,4,5,6})^\perp \cap$span $\{\boldsymbol{\delta}_i^{(1,2)}\}_{i=1,4,5,7,8,9,10,13,14,15}$ and, again in order to make $\delta$ large, we take

$$\boldsymbol{\theta}_1 = \frac{1}{\langle P_{\mathcal{A}_1} \tilde{\boldsymbol{\phi}}_1, \tilde{\boldsymbol{\phi}}_1 \rangle} P_{\mathcal{A}_1} \tilde{\boldsymbol{\phi}}_1.$$

$\boldsymbol{\theta}_2$ and $\boldsymbol{\theta}_3$ are obtained from $\boldsymbol{\theta}_1$ by permuting the barycentric coordinates.

By evaluating the above expressions, we find the coefficients of $\tilde{\boldsymbol{\Phi}}$ and $\boldsymbol{\Theta}$ with respect to $\boldsymbol{\Delta}^{(2,0)}$ and $\boldsymbol{\Delta}^{(1,2)}$ respectively. These coefficients are collected in the appendix. Next, we use $\boldsymbol{\Theta}$ to construct $\boldsymbol{\Xi}$:

Step 4: In view of $(\mathcal{V})$, $\operatorname{span}\{\boldsymbol{\xi}_i\}_{i=13,14,15}$ has to be equal to $\operatorname{span}\{\boldsymbol{\delta}_i^{(1,2)}\}_{i=13,14,15}$. Next, we take $\operatorname{span}\{\boldsymbol{\xi}_7, \boldsymbol{\xi}_9\}$ as follows: Note that

$$\operatorname{span}\{(\boldsymbol{\Xi} \setminus \{\boldsymbol{\xi}_7, \boldsymbol{\xi}_9\}) \cup \boldsymbol{\Theta}\} = \operatorname{span}\{\{\boldsymbol{\delta}_i^{(1,2)}\}_{i=3,5,6,8,10,11,12,13,14,15} \cup \{\boldsymbol{\theta}_i\}_{i=1,2,4}\},$$

hence, in order to make both $\boldsymbol{\epsilon}$ and $\kappa_{\boldsymbol{\Xi}}$ small, we let $\mathcal{A}_7 := \operatorname{span}\{\boldsymbol{\delta}_i^{(1,2)}\}_{i=4,7,9,13,14,15}$ and take

$$\operatorname{span}\{\boldsymbol{\xi}_7, \boldsymbol{\xi}_9\} = P_{\mathcal{A}_7}((\operatorname{span}\{\{\boldsymbol{\delta}_i^{(1,2)}\}_{i=3,5,6,8,10,11,12,13,14,15} \cup \{\boldsymbol{\theta}_i\}_{i=1,2,4}\})^{\perp} \cap P_{1,2}(\boldsymbol{T})).$$

$\operatorname{span}\{\boldsymbol{\xi}_8, \boldsymbol{\xi}_{10}\}$ and $\operatorname{span}\{\boldsymbol{\xi}_{11}, \boldsymbol{\xi}_{12}\}$ are defined from $\operatorname{span}\{\boldsymbol{\xi}_7, \boldsymbol{\xi}_9\}$ by permuting the barycentric coordinates.

Step 5: Finally, in order to make $\kappa_{\boldsymbol{\Xi}}$ small, we construct an orthonormal basis $\{\boldsymbol{\xi}_7, \boldsymbol{\xi}_9\}$ for $\operatorname{span}\{\boldsymbol{\xi}_7, \boldsymbol{\xi}_9\}$ satisfying $(\mathcal{V})$, $(\mathcal{S})$ and $(\mathcal{I})$ analogously to the previous case. Further, we take

$$\begin{pmatrix} \boldsymbol{\xi}_{13} \\ \boldsymbol{\xi}_{14} \\ \boldsymbol{\xi}_{15} \end{pmatrix} = \left[\langle \boldsymbol{\delta}_i^{(1,2)}, \boldsymbol{\delta}_j^{(1,2)} \rangle_{i,j=13,14,15}\right]^{-\frac{1}{2}} \begin{pmatrix} \boldsymbol{\delta}_{13}^{(1,2)} \\ \boldsymbol{\delta}_{14}^{(1,2)} \\ \boldsymbol{\delta}_{15}^{(1,2)} \end{pmatrix},$$

so that $\{\boldsymbol{\xi}_{13}, \boldsymbol{\xi}_{14}, \boldsymbol{\xi}_{15}\}$ is an orthonormal basis for $\operatorname{span}\{\boldsymbol{\delta}_i^{(1,2)}\}_{i=13,14,15}$ satisfying $(\mathcal{V})$, $(\mathcal{S})$ and $(\mathcal{I})$. The resulting $\boldsymbol{\Xi}$ satisfies thus all three conditions $(\mathcal{V})$, $(\mathcal{S})$ and $(\mathcal{I})$, and it holds that $\operatorname{span}\{\boldsymbol{\Theta} \cup \boldsymbol{\Xi}\} = P_{1,2}(\boldsymbol{T})$. The coefficients of $\boldsymbol{\Xi}$ with respect to $\boldsymbol{\Delta}^{(1,2)}$ are collected in the appendix.

3.4. **The case** $(n, d, \tilde{d}) = (1, 2, 5)$**.** In this case, we fix a numbering of $\boldsymbol{I}_{\tilde{d}-1} = \boldsymbol{I}_4$ and $\boldsymbol{I}_{2(\tilde{d}-1)} = \boldsymbol{I}_8$ as in Figure 8, so that we can switch between these numbers and the corresponding barycentric coordinates at our convenience.

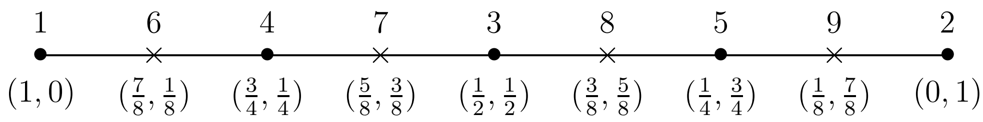


FIGURE 8. Numbering of $\boldsymbol{I}_4$ and $\boldsymbol{I}_8$ ($\bullet \in \boldsymbol{I}_4$, $\times \in \boldsymbol{I}_8 \setminus \boldsymbol{I}_4$), $(n, d, \tilde{d}) = (1, 2, 5)$.

The realization below is carried out analogously to the one in the case $(n, d, \tilde{d}) = (1, 2, 3)$:

Step 1: In view of $(\mathcal{V})$, $\operatorname{span}\{\tilde{\boldsymbol{\phi}}_i\}_{i=3,4,5}$ has to be equal to $\operatorname{span}\{\boldsymbol{\delta}_i^{(4,0)}\}_{i=3,4,5}$. We take $\tilde{\boldsymbol{\phi}}_i = \boldsymbol{\delta}_i^{(4,0)}$ for $i = 3, 4, 5$. In view of making $\kappa_{\tilde{\boldsymbol{\Phi}}}$ as small as possible, it seems more natural to select $\{\tilde{\boldsymbol{\phi}}_i\}_{i=3,4,5}$ as an orthonormal basis. However, as we learn from Remark 2.7, the wavelets $\Psi_j$ do not depend on the choice of the bases $\Theta_j$ and $\tilde{\Phi}_j$ for $\operatorname{span}\Theta_j$ and $\tilde{V}_j$. One may verify that other choices of a basis for $\operatorname{span}\{\tilde{\boldsymbol{\phi}}_i\}_{i=3,4,5}$

do not change $\operatorname{span}\Theta_j$ and $\tilde{V}_j$. In view of an efficient implementation, the above simple choice is the best.

Now we let $\mathcal{A}_3 := \operatorname{span}\{\boldsymbol{\delta}_i^{(1,3)}\}_{i=3,\cdots,9}$ and in order to make $\boldsymbol{\delta}$ large, we take, with $\tilde{\boldsymbol{\Phi}}^{(\mathrm{int})} := \{\tilde{\boldsymbol{\phi}}_i\}_{i=3,4,5}$,

$$\begin{pmatrix} \boldsymbol{\theta}_3 \\ \boldsymbol{\theta}_4 \\ \boldsymbol{\theta}_5 \end{pmatrix} = \langle P_{\mathcal{A}_3}\tilde{\boldsymbol{\Phi}}^{(\mathrm{int})}, \tilde{\boldsymbol{\Phi}}^{(\mathrm{int})}\rangle^{-1} P_{\mathcal{A}_3}\tilde{\boldsymbol{\Phi}}^{(\mathrm{int})}.$$

Note that $\langle \tilde{\boldsymbol{\Phi}}^{(\mathrm{int})}, \boldsymbol{\Theta}^{(\mathrm{int})}\rangle = \mathbf{Id}$.

Step 2: Next, we take, with $\boldsymbol{\Theta}^{(\mathrm{int})} := \{\boldsymbol{\theta}_i\}_{i=3,4,5}$,

$$\tilde{\boldsymbol{\phi}}_1 = \boldsymbol{\delta}_1^{(1,3)} - \langle \boldsymbol{\delta}_1^{(1,3)}, \boldsymbol{\Theta}^{(\mathrm{int})}\rangle \tilde{\boldsymbol{\Phi}}^{(\mathrm{int})}.$$

$\tilde{\boldsymbol{\phi}}_2$ is obtained from $\tilde{\boldsymbol{\phi}}_1$ by permuting the barycentric coordinates. It holds in addition that $\langle \tilde{\boldsymbol{\phi}}_1, \boldsymbol{\Theta}^{(\mathrm{int})}\rangle = \langle \tilde{\boldsymbol{\phi}}_2, \boldsymbol{\Theta}^{(\mathrm{int})}\rangle = 0$.

Step 3: With the above $\tilde{\boldsymbol{\Phi}}$, we let $\mathcal{A}_1 := (\operatorname{span}\{\tilde{\boldsymbol{\phi}}_i\}_{i=2,3,4,5})^\perp \cap \operatorname{span}\{\boldsymbol{\delta}_i^{(1,3)}\}_{i=1,3,\cdots,9}$ and, again in order to make $\boldsymbol{\delta}$ large, we take

$$\boldsymbol{\theta}_1 = \langle P_{\mathcal{A}_1}\tilde{\boldsymbol{\phi}}_1, \tilde{\boldsymbol{\phi}}_1\rangle^{-1} P_{\mathcal{A}_1}\tilde{\boldsymbol{\phi}}_1.$$

$\boldsymbol{\theta}_2$ is obtained from $\boldsymbol{\theta}_1$ by permuting the barycentric coordinates.

By evaluating the above expressions, we find the coefficients of $\tilde{\boldsymbol{\Phi}}$ and $\boldsymbol{\Theta}$ with respect to $\boldsymbol{\Delta}^{(4,0)}$ and $\boldsymbol{\Delta}^{(1,3)}$ respectively. These coefficients are collected in the appendix. Next, we use $\boldsymbol{\Theta}$ to construct $\Xi$:

Step 4: In order to make $\boldsymbol{\epsilon}$ small, we take

$$\operatorname{span}\Xi = P_{\mathcal{A}_3}((\operatorname{span}\boldsymbol{\Theta})^\perp \cap P_{1,3}(\boldsymbol{T}))$$

with $\mathcal{A}_3$ being defined in step 1.

Step 5: Finally, in order to minimize $\kappa_{\boldsymbol{\Xi}}$, we are going to find an orthonormal basis for $\operatorname{span}\Xi$ as follows: Analogously to the case $(n,d,\tilde{d}) = (1,2,3)$, with $\boldsymbol{\Theta}^\perp$ being a basis for $(\operatorname{span}\boldsymbol{\Theta})^\perp \cap P_{1,3}(\boldsymbol{T})$ satisfying $(\mathcal{S})$, then a basis $\Xi^{(0)}$ for $\operatorname{span}\Xi$ satisfying $(\mathcal{S})$ is given by

$$\Xi^{(0)} = \begin{pmatrix} \boldsymbol{\xi}_6^{(0)} \\ \boldsymbol{\xi}_7^{(0)} \\ \boldsymbol{\xi}_8^{(0)} \\ \boldsymbol{\xi}_9^{(0)} \end{pmatrix} = P_{\mathcal{A}_3}\boldsymbol{\Theta}^\perp.$$

Now, if we would have taken

$$\Xi = \langle \Xi^{(0)}, \Xi^{(0)}\rangle^{-\frac{1}{2}}\Xi^{(0)},$$

then, of course, $\Xi$ is an orthonormal basis for $\operatorname{span}\Xi$. However, the elements of $\Xi$ can not be given in closed form in terms of $\boldsymbol{\Delta}^{(1,3)}$.

To solve this problem, we proceed as follows: First we apply an orthogonal basis transformation $\mathbf{U}$ on $\Xi^{(0)}$ to obtain an intermediate basis $\Xi^{(1)}$ such that $\langle \Xi^{(1)}, \Xi^{(1)}\rangle$ is a block diagonal matrix (basically, $\Xi^{(1)}$ consists of functions which are either symmetric or antisymmetric with respect to the barycentric coordinates). Next, we apply the Gram-Schmidt orthonormalization process on $\Xi^{(1)}$ to obtain another intermediate orthonormal basis $\Xi^{(2)}$. Note that, $\Xi^{(2)}$ does not necessarily satisfy $(\mathcal{S})$, since neither does $\Xi^{(1)}$. Hence, we apply $\mathbf{U}^{-1}$ on $\Xi^{(2)}$ to obtain the final orthonormal basis $\Xi$ satisfying $(\mathcal{S})$. Further, $\Xi$ also satisfies $(\mathcal{V})$ and $(\mathcal{I})$, and it holds that span $\{\boldsymbol{\Theta} \cup \boldsymbol{\Xi}\} = P_{1,2}(\boldsymbol{T})$. The coefficients of $\boldsymbol{\Xi}$ with respect to $\boldsymbol{\Delta}^{(1,3)}$ are collected in the appendix.

3.5. **The case** $(n, d, \tilde{d}) = (2, 2, 5)$**.** The realization in this case is based on a combination of the ideas applied in the cases $(n, d, \tilde{d}) = (2, 2, 3)$ and $(n, d, \tilde{d}) = (1, 2, 5)$. We refer to [Ngu05, §3.3] for details.

3.6. **The cases** $(d, \tilde{d}) = (3, 3)$ **and** $(d, \tilde{d}) = (3, 5)$ **for** $n \in \{1, 2\}$**.** The realization in these cases follows the same lines as the corresponding cases $(d, \tilde{d}) = (2, 3)$ and $(d, \tilde{d}) = (2, 5)$ for $n \in \{1, 2\}$ above.

## 4. Numerical results

In this section, we present the numerical results of several one and two dimensional experiments. In our experiments, $\Omega = (0, 1)^n$ for $n = 1, 2$. Further, with

$$T_1 := [0, 1],$$

and

$$\begin{cases} T_{21} := \{x = (x_1, x_2) \in [0, 1]^2 : x_2 \geq x_1\} \\ T_{22} := \{x = (x_1, x_2) \in [0, 1]^2 : x_2 \leq x_1\} \end{cases},$$

$\tau_0$ is the triangulation resulting from the $\log_2(\tilde{d} - 1)$-times repeated uniform dyadic refinement of $\{T_1\}$ and $\{T_{21}, T_{22}\}$ for $n = 1$ and $n = 2$, respectively. In addition, homogeneous Dirichlet boundary conditions on $\partial\Omega$ are incorporated in the spaces $V_j$ and $\tilde{V}_j$ (cf. Remark 2.11).

Recall that, for $j \geq 0$, our collection of wavelets $\Psi_j$ is determined via formulas (2.1) and (2.5) by the local collections $\tilde{\boldsymbol{\Phi}}$, $\boldsymbol{\Theta}$ and $\boldsymbol{\Xi}$ from the previous section. Further, we take $\Psi_{-1} = \Delta_0^{(d-1,p)}$ (recall that $(d - 1)2^p = \tilde{d} - 1$). In addition, for comparison, for $j \geq 0$, let $\tilde{\Phi}_{j,\mathrm{DS}}$, $\Theta_{j,\mathrm{DS}}$ and $\Xi_{j,\mathrm{DS}}$ be the global collections corresponding to the local collections $\tilde{\boldsymbol{\Phi}}$, $\boldsymbol{\Theta}$ and $\boldsymbol{\Xi}$ given in [DS99c], and let

$$\Psi_{j,\mathrm{DS}} := \Xi_{j,\mathrm{DS}} - \langle \Xi_{j,\mathrm{DS}}, \tilde{\Phi}_{j,\mathrm{DS}} \rangle \Theta_{j,\mathrm{DS}}$$

with $\Psi_{-1,\mathrm{DS}} := \Delta_0^{(d-1,p)}$.

Since our main goal is to investigate the condition numbers of the mass matrices with respect to the wavelet bases, *in the rest of this section, instead of* $\Psi_j$ *and* $\Psi_{j,\mathrm{DS}}$ *we consider the* ($L^2$-) *normalized collections for which, for notational simplicity, we will use the same notation* $\Psi_j$ *and* $\Psi_{j,\mathrm{DS}}$.

For $j \geq 0$ being the finest level, let

$$\Psi^{(j)} := \bigcup_{l=-1}^{j-1} \Psi_l.$$

We computed the quantities $\kappa_{\Psi^{(j)}} = \kappa_{L^2,\Psi^{(j)}}$ and $\kappa_{\Psi^{(j)}_{\mathrm{DS}}} = \kappa_{L^2,\Psi^{(j)}_{\mathrm{DS}}}$, with $\Psi^{(j)}_{\mathrm{DS}}$ being defined analogously to $\Psi^{(j)}$. The numerical results for one and two space dimensions with $j = 10$ and $j = 6$ are presented in Table 1. They show that $\kappa_{\Psi^{(j)}}$ (first column) is significantly improved in comparison with $\kappa_{\Psi^{(j)}_{\mathrm{DS}}}$. Since the four cases where $d = 3$ were not considered in [DS99c], in these cases the condition number of $\Psi^{(j)}_{\mathrm{DS}}$ is not present in our tables.

| | $n = 1$ | | $n = 2$ | |
|---|---|---|---|---|
| $(d, \tilde{d})$ | $\kappa_{\Psi^{(10)}}$ | $\kappa_{\Psi^{(10)}_{\mathrm{DS}}}$ | $\kappa_{\Psi^{(6)}}$ | $\kappa_{\Psi^{(6)}_{\mathrm{DS}}}$ |
| $(2, 2)$ | 2.2498e+00 | | 1.2214e+01 | |
| $(2, 3)$ | 5.1018e+00 | 8.6322e+00 | 1.6791e+01 | 1.4741e+02 |
| $(2, 5)$ | 8.9115e+00 | 1.4724e+02 | 2.1829e+01 | 2.1835e+04 |
| $(3, 3)$ | 2.9034e+00 | – | 1.2344e+01 | – |
| $(3, 5)$ | 5.5588e+00 | – | 1.5955e+01 | – |

TABLE 1. $\kappa_{\Psi^{(j)}}$ v.s. $\kappa_{\Psi^{(j)}_{\mathrm{DS}}}$ ($j = 10$ for $n = 1$, and $j = 6$ for $n = 2$)

In order to further assess the quality of our wavelets, we also computed the quantities $\kappa_{\bar{\Psi}^{(j)}} = \kappa_{L^2,\bar{\Psi}^{(j)}}$ and $\kappa_{\Psi_{j-1}} = \kappa_{L^2,\Psi_{j-1}}$, where, for $l \geq -1$,

$$\bar{\Psi}_l := \langle \Psi_l, \Psi_l \rangle^{-\frac{1}{2}} \Psi_l,$$

and $\bar{\Psi}^{(j)} := \cup_{l=-1}^{j-1} \bar{\Psi}_l$. Note that $\bar{\Psi}_l$ are orthonormal bases for the detail spaces $W_l := V_{l+1} \cap \tilde{V}_l^{\perp}$, which, however, are globally supported. The reason for us to compute $\kappa_{\bar{\Psi}^{(j)}}$ and $\kappa_{\Psi_{j-1}}$ is as follows. Since $\bar{\Psi}_l$ is an orthonormal basis for $W_l$, from (1.1) we infer in particular that

$$\kappa_{\Psi^{(j)}} \leq \kappa_{\bar{\Psi}^{(j)}} \frac{\max\limits_{-1 \leq l \leq j-1} \Lambda_{\Psi_l}}{\min\limits_{-1 \leq l \leq j-1} \lambda_{\Psi_l}}. \tag{4.1}$$

Furthermore, for $k \leq l$, $\langle \Psi_k, \Psi_k \rangle$ is a submatrix of $\langle \Psi_l, \Psi_l \rangle$, from which it follows that

$$\Lambda_{\Psi_{j-1}} = \max_{-1 \leq l \leq j-1} \Lambda_{\Psi_l} \quad \text{and} \quad \lambda_{\Psi_{j-1}} = \min_{-1 \leq l \leq j-1} \lambda_{\Psi_l}.$$

Hence, (4.1) reads as

$$\kappa_{\Psi^{(j)}} \leq \kappa_{\bar{\Psi}^{(j)}} \kappa_{\Psi_{j-1}}.$$

Note that $\kappa_{\bar{\Psi}^{(j)}}$ is nothing else than the condition number of the splitting $V_j = \sum_{l=-1}^{j-1} W_l$, and that $\kappa_{\Psi_{j-1}}$ is the condition number of the basis $\Psi_{j-1}$ for the single detail space $W_{j-1}$. The value of $\kappa_{\bar{\Psi}^{(j)}}$ thus shows which condition number will be achieved by equipping $V_j =$

$\sum_{l=-1}^{j-1} W_l$ with a multilevel basis that is the union of orthonormal bases for the detail spaces $W_l$. Since we expect that the condition number of such a multilevel basis is close to the minimal one (although it is not necessarily the minimal one, cf. [Ngu05, §2.1]), we take $\kappa_{\bar{\Psi}^{(j)}}$ as a benchmark.

| | $n=1$ | | | $n=2$ | | |
|---|---|---|---|---|---|---|
| $(d,\tilde{d})$ | $\kappa_{\Psi^{(10)}}$ | $\kappa_{\bar{\Psi}^{(10)}}$ | $\kappa_{\Psi_9}$ | $\kappa_{\Psi^{(6)}}$ | $\kappa_{\bar{\Psi}^{(6)}}$ | $\kappa_{\Psi_5}$ |
| $(2,2)$ | 2.2498e+00 | 1.0027e+00 | 2.2498e+00 | 1.2214e+01 | 1.0039e+00 | 1.2214e+01 |
| $(2,3)$ | 5.1018e+00 | 2.6203e+00 | 2.3021e+00 | 1.6791e+01 | 2.8057e+00 | 9.2045e+00 |
| $(2,5)$ | 8.9115e+00 | 6.5210e+00 | 1.6170e+00 | 2.1829e+01 | 7.8906e+00 | 5.8825e+00 |
| $(3,3)$ | 2.9034e+00 | 1.0026e+00 | 2.9034e+00 | 1.2344e+01 | 1.0043e+00 | 1.2344e+01 |
| $(3,5)$ | 5.5588e+00 | 3.4889e+00 | 1.7769e+00 | 1.5955e+01 | 5.8180e+00 | 6.7210e+00 |

TABLE 2. $\kappa_{\Psi^{(j)}}$ v.s. $\kappa_{\bar{\Psi}^{(j)}}$ ($j=10$ for $n=1$, and $j=6$ for $n=2$)

From the results given in Table 2, we draw the following conclusions:

- The bases $\Psi^{(j)}$ are quite well-conditioned in comparison with the bases $\bar{\Psi}^{(j)}$.
- There is not much room left for improving $\kappa_{\Psi^{(j)}}$ by some post processing aiming at constructing better conditioned bases for the detail spaces $W_l$ (e.g., level-wise orthonormalization). Moreover, such a post processing likely results in wavelets with larger supports.
- The bases $\Psi_l$ have small condition numbers. In particular, it appears that the more freedom there exist in the construction, due to a larger $\tilde{d}$, the better conditioned the resulting wavelet bases are (specially in one dimension, cf. the cases $(n,d,\tilde{d}) = (1,2,5)$ and $(n,d,\tilde{d}) = (1,3,5)$).
- Finally, the upper bound in (4.1) is rather sharp in all cases we considered.

We conclude this section with the $H^1$-condition numbers of the $H^1$-normalized multilevel wavelet bases presented in Table 3. For notational simplicity, those bases are also denoted by $\Psi^{(j)}$ and $\Psi^{(j)}_{\mathrm{DS}}$.

| | $n=1$ | | $n=2$ | |
|---|---|---|---|---|
| $(d,\tilde{d})$ | $\kappa_{H^1,\Psi^{(10)}}$ | $\kappa_{H^1,\Psi^{(10)}_{\mathrm{DS}}}$ | $\kappa_{H^1,\Psi^{(6)}}$ | $\kappa_{H^1,\Psi^{(6)}_{\mathrm{DS}}}$ |
| $(2,2)$ | 1.5536e+01 | | 4.8632e+01 | |
| $(2,3)$ | 1.0217e+01 | 3.7198e+01 | 5.1059e+01 | 3.0274e+02 |
| $(2,5)$ | 1.5207e+01 | 6.4225e+02 | 5.9284e+01 | 3.3645e+04 |
| $(3,3)$ | 9.3342e+00 | – | 5.9916e+01 | – |
| $(3,5)$ | 1.4422e+01 | – | 5.9729e+01 | – |

TABLE 3. $\kappa_{H^1,\Psi^{(j)}}$ v.s. $\kappa_{H^1,\Psi^{(j)}_{\mathrm{DS}}}$ ($j=10$ for $n=1$, and $j=6$ for $n=2$)

**Remark 4.1.** *In this remark, we briefly explain how we computed the $L^2$-condition numbers given above ($H^1$-condition numbers are computed analogously). Due to the $L^2$-normalization that we applied, one of our tasks is to compute the extremal eigenvalues of a matrix of type*

$$\mathrm{diag}(\mathbf{A}_j)^{-\frac{1}{2}}\mathbf{A}_j\mathrm{diag}(\mathbf{A}_j)^{-\frac{1}{2}},$$

*for which we used the Lanczos method. For computing $\kappa_{\Psi^{(j)}}$ (and analogously for $\kappa_{\Psi^{(j)}_{\mathrm{DS}}}$), the matrix $\mathbf{A}_j$ is given by*

$$\mathbf{A}_j := \langle \Psi^{(j)}, \Psi^{(j)} \rangle = \mathbf{T}_j^T \langle \Delta_j, \Delta_j \rangle \mathbf{T}_j,$$

*where $\Psi^{(j)}$ and $\mathbf{T}_j$ are such that $(\Psi^{(j)})^T := \cup_{l=-1}^{j-1}\Psi_l = \Delta_j^T \mathbf{T}_j$. For computing $\kappa_{\Psi_{j-1}}$, the matrix $\mathbf{A}_j$ is given by*

$$\mathbf{A}_j := \langle \Psi_{j-1}, \Psi_{j-1} \rangle = \mathbf{M}_{\Psi_{j-1}}^T \langle \Delta_j, \Delta_j \rangle \mathbf{M}_{\Psi_{j-1}},$$

*where $\mathbf{M}_{\Psi_{j-1}}$ is such that $\Psi_{j-1}^T = \Delta_j^T \mathbf{M}_{\Psi_{j-1}}$.*

*Finally, with $\mathbf{D}^{(j)} := \mathrm{block\,diag}\,(\langle \Psi_l, \Psi_l \rangle)_{-1 \le l \le j-1}$, we computed $\kappa_{\bar{\Psi}^{(j)}}$ as follows: Instead of applying the Lanczos method on $[(\mathbf{D}^{(j)})^{-\frac{1}{2}}\langle \Psi^{(j)}, \Psi^{(j)}\rangle(\mathbf{D}^{(j)})^{-\frac{1}{2}}]$ using the Euclidean inner product $\langle \cdot, \cdot \rangle$, we applied the Lanczos method on $[(\mathbf{D}^{(j)})^{-1}\langle \Psi^{(j)}, \Psi^{(j)}\rangle]$ using the energy inner product $\langle \cdot, \langle \Psi^{(j)}, \Psi^{(j)} \rangle \cdot \rangle$. In addition, we used Richardson iterations to approximate $(\mathbf{D}^{(j)})^{-1}$. As we observed from our experiments, the error due to Richardson approximations dominates the error due to Lanczos approximations and it is visible in the cases $(d, \tilde{d}) = (2, 2)$ and $(d, \tilde{d}) = (3, 3)$ (for $n \in \{1, 2\}$). Indeed, these cases correspond to an $L^2$-orthogonal splitting, so that $\kappa_{\bar{\Psi}^{(j)}} = 1$ for all $j$.*

## Appendix

In this appendix, we collected the coefficients of $\tilde{\mathbf{\Phi}}$ and $\mathbf{\Theta} \cup \mathbf{\Xi}$ for several cases considered in Section 3. Because of their lengthy expressions we have omitted the coefficients for the remaining cases. They can be obtained by contacting the authors.

**The case** $(n, d, \tilde{d}) = (1, 2, 3)$**.** By evaluating the expressions found in section 3, we find

$$\begin{pmatrix} \tilde{\boldsymbol{\phi}}_1 \\ \tilde{\boldsymbol{\phi}}_3 \end{pmatrix}^T = (\mathbf{\Delta}^{(2,0)})^T \begin{bmatrix} 1 & 0 \\ 0 & 0 \\ -\frac{43}{358} & 1 \end{bmatrix}$$

and

$$\begin{pmatrix} \alpha\boldsymbol{\theta}_1 \\ \alpha\boldsymbol{\theta}_3 \\ \boldsymbol{\xi}_4 \end{pmatrix}^T = (\mathbf{\Delta}^{(1,2)})^T \begin{bmatrix} \frac{59}{6} & 0 & 0 \\ 0 & 0 & 0 \\ -\frac{113}{36} & \frac{348}{179} & -\frac{17}{358}\sqrt{1074} \\ \frac{73}{72} & \frac{270}{179} & \frac{23}{716}\sqrt{1074} + \frac{1}{2}\sqrt{6} \\ \frac{29}{24} & \frac{270}{179} & \frac{23}{716}\sqrt{1074} - \frac{1}{2}\sqrt{6} \end{bmatrix}$$

where $\alpha = \sqrt{2}$. The remaining $\tilde{\boldsymbol{\phi}}_2$, $\boldsymbol{\theta}_2$ and $\boldsymbol{\xi}_5$ are obtained by permuting the barycentric coordinates. The resulting $\tilde{\mathbf{\Phi}}$, $\mathbf{\Theta}$ and $\mathbf{\Theta}$ are illustrated in Figure 9. Some corresponding global functions and wavelets are illustrated in Figure 10 (see Remark 2.11 for the case of wavelets near Dirichlet boundary). Note that the global functions corresponding to $\boldsymbol{\theta}_3$ are not used in the wavelet construction, since we happen to have $\langle \boldsymbol{\xi}_4, \tilde{\boldsymbol{\phi}}_3\rangle = \langle \boldsymbol{\xi}_5, \tilde{\boldsymbol{\phi}}_3\rangle = 0$.

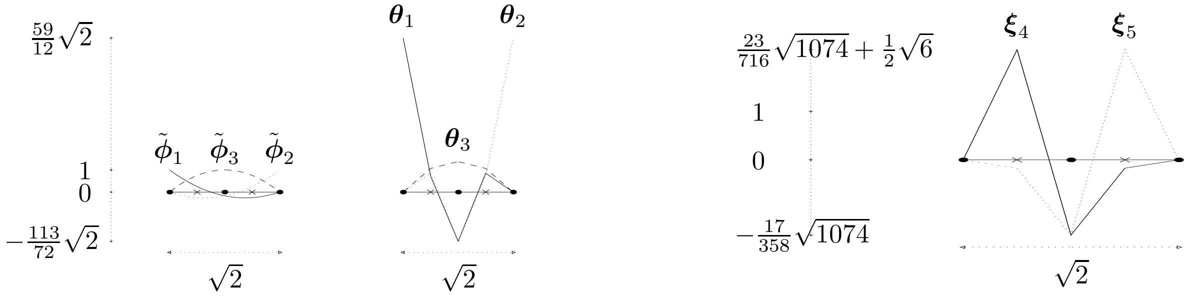


FIGURE 9. $\tilde{\boldsymbol{\Phi}}$, $\boldsymbol{\Theta}$ and $\boldsymbol{\Xi}$ for $(n, d, \tilde{d}) = (1, 2, 3)$.

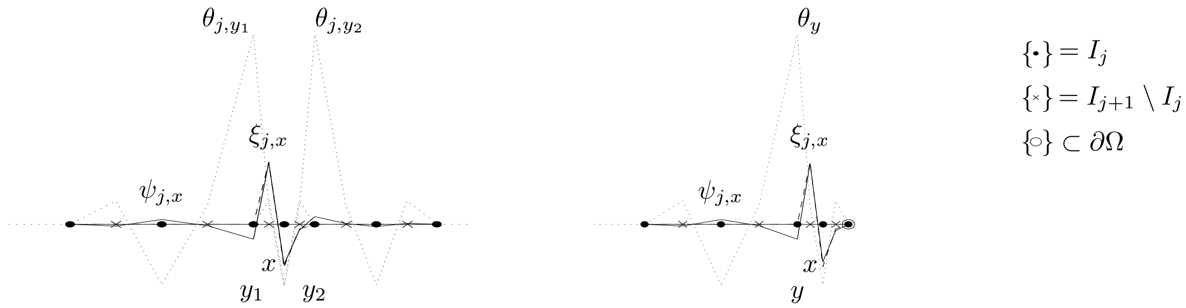


FIGURE 10. $\xi_{j,x}$'s, $\theta_{j,y}$'s and $\psi_{j,x}$'s for $(n, d, \tilde{d}) = (1, 2, 3)$ (right: near Dirichlet boundary).

**The case $(n, d, \tilde{d}) = (2, 2, 3)$.** By evaluating the expressions found in section 3, we find

$$\begin{pmatrix} \tilde{\boldsymbol{\phi}}_1 \\ \tilde{\boldsymbol{\phi}}_6 \end{pmatrix}^T = (\boldsymbol{\Delta}^{(2,0)})^T \begin{bmatrix} 1 & 0 \\ 0 & 0 \\ 0 & 0 \\ -\frac{2393}{21566} & 0 \\ -\frac{2393}{21566} & 0 \\ 0 & 1 \end{bmatrix}$$

and

$$\begin{pmatrix} \alpha\boldsymbol{\theta}_1 \\ \alpha\boldsymbol{\theta}_6 \\ \boldsymbol{\xi}_7 \\ \boldsymbol{\xi}_{13} \end{pmatrix}^T = (\boldsymbol{\Delta}^{(1,2)})^T \begin{bmatrix} \frac{18213930}{198671} & 0 & 0 & 0 \\ 0 & 0 & 0 & 0 \\ 0 & 0 & 0 & 0 \\ -\frac{3905291}{198671} & 0 & -\frac{331388}{2376092663409739}\alpha_1 & 0 \\ -\frac{3905291}{198671} & 0 & 0 & 0 \\ 0 & \frac{408128}{10783} & 0 & 0 \\ \frac{8925711}{397342} & 0 & \frac{28}{216421592441}\alpha_1 + \frac{2}{7}\alpha_2 & 0 \\ \frac{8925711}{397342} & 0 & 0 & 0 \\ \frac{2014981}{397342} & 0 & \frac{28}{216421592441}\alpha_1 - \frac{2}{7}\alpha_2 & 0 \\ \frac{2014981}{397342} & 0 & 0 & 0 \\ 0 & \frac{182432}{10783} & 0 & 0 \\ 0 & \frac{182432}{10783} & 0 & 0 \\ -\frac{2812507}{198671} & \frac{46848}{10783} & \frac{17982}{11880463317048695}\alpha_1 - \frac{2}{35}\alpha_2 & \frac{2}{3}\alpha_3 + \frac{16}{15}\alpha_4 \\ \frac{1390533}{397342} & -\frac{111264}{10783} & \frac{17982}{11880463317048695}\alpha_1 + \frac{2}{35}\alpha_2 & \frac{2}{3}\alpha_3 - \frac{8}{15}\alpha_4 \\ \frac{1390533}{397342} & -\frac{111264}{10783} & -\frac{5994}{11880463317048695}\alpha_1 & \frac{2}{3}\alpha_3 - \frac{8}{15}\alpha_4 \end{bmatrix}$$

where $\alpha = \frac{1}{2}\sqrt{3}$, $\alpha_1 = \sqrt{782613640547265734430}$, $\alpha_2 = \sqrt{210}$, $\alpha_3 = \sqrt{6}$ and $\alpha_4 = \sqrt{15}$. The remaining $\tilde{\boldsymbol{\phi}}_i$, $\boldsymbol{\theta}_i$ and $\boldsymbol{\xi}_i$ are obtained by permuting the barycentric coordinates.

**The case** $(n, d, \tilde{d}) = (1, 3, 3)$**.** By evaluating the expressions found in section 3, we find

$$\begin{pmatrix} \tilde{\boldsymbol{\phi}}_1 \\ \tilde{\boldsymbol{\phi}}_3 \end{pmatrix}^T = (\boldsymbol{\Delta}^{(2,0)})^T \begin{bmatrix} 1 & 0 \\ 0 & 0 \\ -\frac{1}{8} & 1 \end{bmatrix}$$

and

$$\begin{pmatrix} \alpha\boldsymbol{\theta}_1 \\ \alpha\boldsymbol{\theta}_3 \\ \boldsymbol{\xi}_4 \end{pmatrix}^T = (\boldsymbol{\Delta}^{(2,1)})^T \begin{bmatrix} \frac{39}{4} & 0 & 0 \\ 0 & 0 & 0 \\ -\frac{51}{16} & \frac{15}{8} & -\frac{7}{4} \\ \frac{105}{64} & \frac{45}{32} & \frac{11}{16} + \frac{1}{4}\sqrt{15} \\ \frac{33}{64} & \frac{45}{32} & \frac{11}{16} - \frac{1}{4}\sqrt{15} \end{bmatrix}$$

where $\alpha = \sqrt{2}$. The remaining $\tilde{\boldsymbol{\phi}}_2$, $\boldsymbol{\theta}_2$ and $\boldsymbol{\xi}_5$ are obtained by permuting the barycentric coordinates.

**The case** $(n, d, \tilde{d}) = (2, 3, 3)$**.** By evaluating the expressions found in section 3, we find

$$\begin{pmatrix} \tilde{\boldsymbol{\phi}}_1 \\ \tilde{\boldsymbol{\phi}}_6 \end{pmatrix}^T = (\boldsymbol{\Delta}^{(2,0)})^T \begin{bmatrix} 1 & 0 \\ 0 & 0 \\ 0 & 0 \\ -\frac{7}{100} & 0 \\ -\frac{7}{100} & 0 \\ 0 & 1 \end{bmatrix}$$

and

$$\begin{pmatrix} \alpha\boldsymbol{\theta}_1 \\ \alpha\boldsymbol{\theta}_6 \\ \boldsymbol{\xi}_7 \\ \boldsymbol{\xi}_{13} \end{pmatrix}^T = (\boldsymbol{\Delta}^{(2,1)})^T \begin{bmatrix} \frac{29148}{379} & 0 & 0 & 0 \\ 0 & 0 & 0 & 0 \\ 0 & 0 & 0 & 0 \\ -\frac{10752}{379} & 0 & -\frac{3812}{731985681}\alpha_1 & 0 \\ -\frac{10752}{379} & 0 & 0 & 0 \\ 0 & \frac{954}{25} & 0 & 0 \\ \frac{17955}{758} & 0 & \frac{25}{6564894}\alpha_1 + \frac{3}{2}\alpha_2 & 0 \\ \frac{17955}{758} & 0 & 0 & 0 \\ \frac{2499}{758} & 0 & \frac{25}{6564894}\alpha_1 - \frac{3}{2}\alpha_2 & 0 \\ \frac{2499}{758} & 0 & 0 & 0 \\ 0 & \frac{819}{50} & 0 & 0 \\ 0 & \frac{819}{50} & 0 & 0 \\ -\frac{3030}{379} & \frac{189}{50} & -\frac{1133}{1463971362}\alpha_1 - \frac{1}{2}\alpha_2 & \frac{1}{3}\alpha_3 + \frac{2}{3}\alpha_4 \\ -\frac{2649}{758} & -\frac{81}{25} & -\frac{1133}{1463971362}\alpha_1 + \frac{1}{2}\alpha_2 & \frac{1}{3}\alpha_3 - \frac{1}{3}\alpha_4 \\ -\frac{2649}{758} & -\frac{81}{25} & \frac{15}{243995227}\alpha_1 & \frac{1}{3}\alpha_3 - \frac{1}{3}\alpha_4 \end{bmatrix}$$

where $\alpha = \frac{1}{2}\sqrt{3}$, $\alpha_1 = \sqrt{5441093356210}$, $\alpha_2 = \sqrt{6}$, $\alpha_3 = \sqrt{15}$ and $\alpha_4 = \sqrt{30}$. The remaining $\tilde{\boldsymbol{\phi}}_i$, $\boldsymbol{\theta}_i$ and $\boldsymbol{\xi}_i$ are obtained by permuting the barycentric coordinates.

**The case $(n, d, \tilde{d}) = (1, 2, 5)$.** By evaluating the expressions found in section 3, we find

$$\begin{pmatrix} \tilde{\boldsymbol{\phi}}_1 \\ \tilde{\boldsymbol{\phi}}_3 \\ \tilde{\boldsymbol{\phi}}_4 \end{pmatrix}^T = (\boldsymbol{\Delta}^{(4,0)})^T \begin{bmatrix} 1 & 0 & 0 \\ 0 & 0 & 0 \\ -\frac{18739862235}{133516792844} & 1 & 0 \\ \frac{872676719}{133516792844} & 0 & 1 \\ \frac{874703}{17219086} & 0 & 0 \end{bmatrix},$$

$$\begin{pmatrix} \alpha\boldsymbol{\theta}_1 \\ \alpha\boldsymbol{\theta}_3 \\ \alpha\boldsymbol{\theta}_4 \end{pmatrix}^T = (\boldsymbol{\Delta}^{(1,3)})^T \begin{bmatrix} \frac{7227950}{298759} & 0 & 0 \\ 0 & 0 & 0 \\ \frac{39785291}{13444155} & \frac{29685248}{8609543} & \frac{4697536}{8609543} \\ -\frac{125270207}{26888310} & \frac{5358320}{8609543} & \frac{114660586332}{33379198211} \\ -\frac{2240137}{597518} & \frac{5358320}{8609543} & -\frac{13173908132}{33379198211} \\ -\frac{83640971}{53776620} & -\frac{11663656}{8609543} & \frac{121759112646}{33379198211} \\ -\frac{3907307}{17925540} & \frac{22402072}{8609543} & \frac{68957288438}{33379198211} \\ \frac{100172569}{53776620} & \frac{22402072}{8609543} & -\frac{10939270602}{33379198211} \\ \frac{22633121}{17925540} & -\frac{11663656}{8609543} & \frac{3291800966}{33379198211} \end{bmatrix}$$

and

$$\begin{pmatrix} \boldsymbol{\xi}_6 \\ \boldsymbol{\xi}_7 \end{pmatrix}^T = (\boldsymbol{\Delta}^{(1,3)})^T \begin{bmatrix} 0 & 0 \\ 0 & 0 \\ \frac{5270}{120098669021}\alpha_1 & -\frac{27571598}{194982963450701}\alpha_3 \\ -\frac{6588}{120098669021}\alpha_1 - \frac{39}{1370}\alpha_2 & -\frac{12340186}{194982963450701}\alpha_3 - \frac{2863}{5311490}\alpha_4 \\ -\frac{6588}{120098669021}\alpha_1 + \frac{39}{1370}\alpha_2 & -\frac{12340186}{194982963450701}\alpha_3 + \frac{2863}{5311490}\alpha_4 \\ \frac{1}{22647307}\alpha_1 + \frac{23}{685}\alpha_2 & \frac{4151068}{194982963450701}\alpha_3 - \frac{349}{2655745}\alpha_4 \\ 0 & \frac{1}{8609543}\alpha_3 + \frac{4}{3877}\alpha_4 \\ 0 & \frac{1}{8609543}\alpha_3 - \frac{4}{3877}\alpha_4 \\ \frac{1}{22647307}\alpha_1 - \frac{23}{685}\alpha_2 & \frac{4151068}{194982963450701}\alpha_3 + \frac{349}{2655745}\alpha_4 \end{bmatrix}$$

where $\alpha = \sqrt{2}$, $\alpha_1 = \sqrt{636883241818363}$, $\alpha_2 = \sqrt{2055}$, $\alpha_3 = \sqrt{194982963450701}$ and $\alpha_4 = \sqrt{2655745}$. The remaining $\tilde{\boldsymbol{\phi}}_i$, $\boldsymbol{\theta}_i$ and $\boldsymbol{\xi}_i$ are obtained by permuting the barycentric coordinates.

## References


[CDD01] A. Cohen, W. Dahmen, and R. DeVore. Adaptive wavelet methods for elliptic operator equations – Convergence rates. *Math. Comp*, 70:27–75, 2001.

[CDD02] A. Cohen, W. Dahmen, and R. DeVore. Adaptive wavelet methods II - Beyond the elliptic case. *Found. Comput. Math.*, 2(3):203–245, 2002.

[CDF92] A. Cohen, I. Daubechies, and J-C. Feauveau. Biorthogonal bases of compactly supported wavelets. *Comm. Pure Appl. Math.*, 45(5):485–560, 1992.

[CDP96] J. M. Carnicer, W. Dahmen, and J. M. Peña. Local decomposition of refinable spaces and wavelets. *Appl. Comput. Harmon. Anal.*, 3(2):127–153, 1996.

[CDV93] A. Cohen, I. Daubechies, and P. Vial. Wavelets on the interval and fast wavelet transforms. *Appl. Comput. Harmon. Anal.*, 1(1):54–81, 1993.

[CES00] A. Cohen, L-M. Echeverry, and Q. Sun. Finite element wavelets. Technical report, Laboratoire d'Analyse Numérique, Université Pierre et Marie Curie, 2000.

[CM00] A. Cohen and R. Masson. Wavelet adaptive method for second order elliptic problems: boundary conditions and domain decomposition. *Numer. Math.*, 86(2):193–238, 2000.

[Coh03] A. Cohen. *Numerical analysis of wavelet methods*, volume 32 of *Studies in Mathematics and its Applications*. North-Holland Publishing Co., Amsterdam, 2003.

[CQ92] C.K. Chui and E.G. Quak. Wavelets on a bounded interval. In *Numerical methods in approximation theory, Vol. 9 (Oberwolfach, 1991)*, volume 105 of *Internat. Ser. Numer. Math.*, pages 53–75. Birkhäuser, Basel, 1992.

[CTU99] C. Canuto, A. Tabacco, and K. Urban. The wavelet element method. I. Construction and analysis. *Appl. Comput. Harmon. Anal.*, 6(1):1–52, 1999.

[CTU00] C. Canuto, A. Tabacco, and K. Urban. The wavelet element method. II. Realization and additional features in 2D and 3D. *Appl. Comput. Harmon. Anal.*, 8(2):123–165, 2000.

[Dah96] W. Dahmen. Stability of multiscale transformations. *J. Fourier Anal. Appl.*, 2(4):341–361, 1996.

[Dah97] W. Dahmen. Wavelet and multiscale methods for operator equations. In *Acta numerica, 1997*, volume 6 of *Acta Numer.*, pages 55–228. Cambridge Univ. Press, Cambridge, 1997.

[Dau92] I. Daubechies. *Ten lectures on wavelets*, volume 61 of *CBMS-NSF Regional Conference Series in Applied Mathematics*. Society for Industrial and Applied Mathematics, Philadelphia, PA, 1992.

[DKU99] W. Dahmen, A. Kunoth, and K. Urban. Biorthogonal spline wavelets on the interval—stability and moment conditions. *Appl. Comput. Harmon. Anal.*, 6(2):132–196, 1999.

[DS99a] W. Dahmen and R. Schneider. Composite wavelet bases for operator equations. *Math. Comp.*, 68(228):1533–1567, 1999.

[DS99b] W. Dahmen and R. Schneider. Wavelets on manifolds. I. Construction and domain decomposition. *SIAM J. Math. Anal.*, 31(1):184–230 (electronic), 1999.

[DS99c] W. Dahmen and R. Stevenson. Element-by-element construction of wavelets satisfying stability and moment conditions. *SIAM J. Numer. Anal.*, 37(1):319–352 (electronic), 1999.

[FQ00] M.S. Floater and E.G. Quak. Linear independence and stability of piecewise linear prewavelets on arbitrary triangulations. *SIAM J. Numer. Anal.*, 38(1):58–79 (electronic), 2000.

[HS06] H. Harbrecht and R. Stevenson. Wavelets with patchwise cancellation properties. *Math. Comp.*, 75:1871–1889, 2006.

[KO95] U. Kotyczka and P. Oswald. Piecewise linear prewavelets of small support. In *Approximation theory VIII, Vol. 2 (College Station, TX, 1995)*, volume 6 of *Ser. Approx. Decompos.*, pages 235–242. World Sci. Publishing, River Edge, NJ, 1995.

[KS06] A. Kunoth and J. Sahner. Wavelets on manifolds: An optimized construction. *Math. Comp.*, 75:1319–1349, 2006.

[Ngu05] H. Nguyen. *Finite element wavelets for solving partial differential equations.* PhD thesis, Utrecht University, 2005.

[Osw94] P. Oswald. *Multilevel finite element approximation.* Teubner Skripten zur Numerik. [Teubner Scripts on Numerical Mathematics]. B.G. Teubner, Stuttgart, 1994. Theory and applications.

[Sch98] R. Schneider. *Multiskalen- und Wavelet-Matrixkompression: Analysisbasierte Methoden zur effizienten Lösung großer vollbesetzter Gleigungssysteme.* Advances in Numerical Mathematics. B.G. Teubner, Stuttgart, 1998.

[Ste98] R. Stevenson. Piecewise linear (pre-)wavelets on non-uniform meshes. In *Multigrid methods V (Stuttgart, 1996)*, volume 3 of *Lect. Comput. Sci. Eng.*, pages 306–319. Springer, Berlin, 1998.

[Ste03] R. Stevenson. Locally supported, piecewise polynomial biorthogonal wavelets on nonuniform meshes. *Constr. Approx.*, 19(4):477–508, 2003.

[Ste04] R. Stevenson. On the compressibility operators in wavelet coordinates. *SIAM J. Math. Anal.*, 35(5):1110–1132 (electronic), 2004.

[Ste07] R. Stevenson. Composite wavelet bases with extended stability and cancellation properties. *SIAM J. Numer. Anal.*, 45(1):133–162, 2007.

Department of Science and Technology, Linköping University, Campus Norrköping, SE-601 74 Norrköping, Sweden.

*E-mail address*: `hoang@itn.liu.se`

Department of Mathematics, Utrecht University, P.O. Box 80.010, NL-3508 TA Utrecht, The Netherlands.

*E-mail address*: `stevenson@math.uu.nl`